Supporting Information

<u>Contents</u>

1. Instrumentation and Materials

Commercially available solvents and reagents were used without further purification unless otherwise noted. Dry dichloromethane was distilled over CaH_2. The spectroscopic grade solvents were used as solvents for all spectroscopic studies. Silica gel column chromatography was performed on Wakogel C-300. Alumina column chromatography was performed on Sumitomo γ-Alumina. Thin-layer chromatography (TLC) was carried out on aluminum sheets coated with silica gel 60 F254 (Merck 5554). UV/Visible absorption spectra were recorded on Shimadzu UV-3600 spectrometers. ^{1}H and ^{13}C NMR spectra were recorded on a JEOL ECA-600 spectrometer (operating as 600 MHz for ^{1}H and 151 MHz for ^{13}C) using the residual solvent as the internal reference for ^{1}H (δ = 7.26 ppm in $CDCl_3$) and for ^{13}C (δ = 77.16 ppm in $CDCl_3$). Mass spectra were recorded on a BRUKER micrOTOF model using positive and negative mode and a Shimadzu AXIMA-CFRplus using positive-MALDI-TOF method with matrix. Single-crystal diffraction analysis data were collected at –180 °C with a Rigaku XtaLAB P200 by using graphite monochromated Cu-K_α radiation (λ = 1.54187 Å). The structures were solved by direct methods (SHELXS-97) and refined with full-matrix least square technique (SHELXL-97). Redox potentials were measured on an ALS electrochemical analyzer model 660.

2. Experimental Section

2.1 **1M** and **4M** were synthesized according to ref. S1-4.

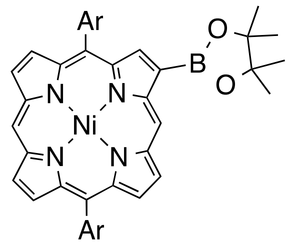

Ar = 3,5-di-*tert*-butylphenyl

1Ni

1Ni; ^{1}H NMR ($CDCl_3$, r.t.) δ (ppm): 10.63 (s, 1H, por-*meso*), 9.87 (s, 1H, por-*meso*), 9.53 (s, 1H, por-β), 9.26 (d, J = 4.8 Hz, 1H, por-β), 9.16 (d, J = 4.2 Hz, 1H, por-β), 9.14 (d, J = 4.2 Hz, 1H, por-β), 8.97 (overlapping d, J = 4.2 Hz, J = 4.2 Hz, 2H, por-β), 8.92 (d, J = 4.8 Hz, 1H, por-β), 7.93 (d, J = 1.8 Hz, 2H, aryl-*ortho*), 7.91 (d, J = 1.8 Hz, 2H, aryl-*ortho*), 7.77 (t, J = 1.8 Hz, 1H, aryl-*para*), 7.76 (t, J = 1.8 Hz, 1H, aryl-*para*), 1.64 (s, 12H, pinacol borate-methyl), and 1.52 (s, 36H, *t*Bu); ^{13}C NMR ($CDCl_3$) δ (ppm): 149.2, 149.0, 146.3, 143.7, 143.5, 143.3, 143.2, 143.1, 143.0, 142.8, 142.5, 140.2, 140.1, 133.0, 132.8, 132.6, 132.1, 131.7, 129.3, 129.2, 126.5, 121.4, 121.2, 120.4, 119.3, 106.4, 104.8, 84.2, 35.2, 31.9, and 25.3; HR-APCI-TOF-MS *m/z* = 868.4480, calcd. for $C_{54}H_{64}N_4{}^{10}B_1{}^{58}Ni_1O_2$ = 868.4507 $[M+H]^+$; UV/Vis (CH_2Cl_2): λ_{max} (ε)= 408 (212000), 520 (13000) and 553 nm (5000 $M^{-1}cm^{-1}$).

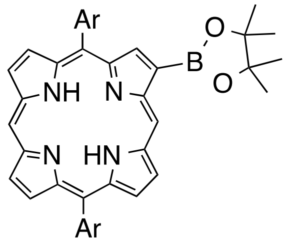

Ar = 3,5-di-*tert*-butylphenyl

1H

1H; ^{1}H NMR ($CDCl_3$, r.t.) δ (ppm): 11.02 (s, 1H, por-*meso*), 10.26 (s, 1H, por-*meso*), 9.68 (s, 1H, por-β), 9.48 (d, J = 4.2 Hz, 1H, por-β), 9.38 (d, J = 4.2 Hz, 1H, por-β), 9.36 (d, J = 4.8 Hz, 1H, por-β), 9.13 (overlapping d, J = 4.2 Hz, J = 4.2 Hz, 1H+1H, por-β), 9.08 (d, J = 4.8 Hz, 1H, por-β), 8.16 (d, J = 1.8 Hz, 2H, aryl-*ortho*), 8.14 (d, J = 1.8 Hz, 2H, aryl-*ortho*), 7.85 (m, 2H, aryl-*para*), 1.71 (s, 12H, pinacol borate-methyl), 1.59 (s, 36H, *t*Bu), and –2.87 (s, 2H, inner *N*H); ^{13}C NMR ($CDCl_3$) δ (ppm): 149.3, 149.1, 148.4, 147.5, 146.0, 145.0, 141.8, 140.63, 140.60, 132.9, 131.8, 131.6, 131.5, 131.30, 131.28, 130.43, 130.37, 121.3, 121.2, 120.1, 106.9, 106.8, 104.9, 84.4, 35.3, 32.0, and 25.4; HR-APCI-TOF-MS *m/z* =812.5336, calcd. for $C_{54}H_{66}N_4{}^{10}B_1O_2$ = 812.5310 $[M+H]^+$; UV/Vis (CH_2Cl_2):□ λ_{max} (ε)= 414 (415000), 509 (17000), 544 (6000), 583 (6000) and 638 nm (3000 $M^{-1}cm^{-1}$).

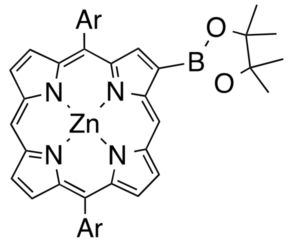

Ar = 3,5-di-*tert*-butylphenyl

1Zn

1Zn; ^{1}H NMR ($CDCl_3$, r.t.) δ (ppm): 11.04 (s, 1H, por-*meso*), 10.29 (s, 1H, por-*meso*), 9.78 (s, 1H, por-β), 9.55 (d, J = 4.2 Hz, 1H, por-β), 9.44 (d, J = 4.8 Hz, 1H, por-β), 9.42 (d, J = 4.8 Hz, 1H, por-β), 9.20 (d, J = 4.8 Hz, 1H, por-β), 9.19 (d, J = 4.8 Hz, 1H, por-β), 9.15 (d, J = 4.2 Hz, 1H, por-β), 8.16 (d, J = 1.8 Hz, 2H, aryl-*ortho*), 8.14 (d, J = 1.8 Hz, 2H, aryl-*ortho*), 7.85 (m, 2H, aryl-*para*), 1.71 (s, 12H, pinacol borate-methyl), and 1.59 (s, 36H, *t*Bu); ^{13}C NMR ($CDCl_3$) δ (ppm): 153.2, 151.2, 151.0, 150.4, 150.0, 149.8, 149.7, 148.9, 148.8, 143.4, 141.7, 133.2, 133.0, 132.9, 132.7, 131.9, 131.6, 130.3, 130.1, 122.3, 121.2, 121.1, 121.0, 107.9, 106.0, 84.2, 35.2, 32.0, and 25.4; HR-APCI-TOF-MS m/z = 874.4402, calcd. for $C_{54}H_{64}N_4{}^{10}B_1{}^{64}Zn_1O_2$= 874.4445 [$M$+H]$^+$; UV/Vis ($CH_2Cl_2$): λ_{max} (ε)= 414 (488000), 542 (23000) and 582 nm (9000 $M^{-1}cm^{-1}$).

2.2 General procedure for the synthesis of 2M.

1M (0.10 mmol), Pt(cod)Cl_2 (18.7 mg, 0.05 mmol), cod (0.20 mL, 1.63 mmol) and CsF (91.0 mg, 0.6 mmol) in THF (7.5 mL) was stirred at reflux for 24 hours under inert atmosphere. Then the mixture was cooled down to room temperature and THF was removed under vacuum. The residue was dissolved in small amount of CH_2Cl_2 and was subjected onto a column chromatography on silica using CH_2Cl_2/hexane (v/v=1/1) as an eluent to give two bands. The second band was collected as the desired compound **2M**.

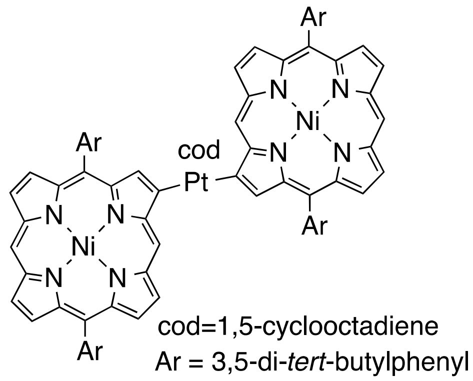

2Ni

2Ni; 75.1 mg, 84% yield; ^{1}H NMR ($CDCl_3$, r.t.) δ (ppm): 10.66 (s, 2H, por-*meso*), 9.67 (s, 2H, por-*meso*), 9.12 (s, 2H, por-β), 8.98 (d, J = 4.8 Hz, 2H, por-β), 8.95 (d, J = 4.8 Hz, 2H, por-β), 8.94 (d, J = 4.8 Hz, 2H, por-β), 8.81 (d, J = 4.8 Hz, 2H, por-β), 8.76 (d, J = 4.8 Hz, 2H, por-β), 8.69 (d, J = 4.8 Hz, 2H, por-β), 7.81 (m, 4H, aryl-*ortho*), 7.77 (m, 4H, aryl-*ortho*), 7.76 (m, 2H, aryl-*para*), 7.70 (m, 2H, aryl-*para*), 5.88 (m, 4H, cod), 3.08 (m, 4H, cod), 2.84 (m, 4H, cod), 1.46 (s, 36H, *t*Bu), and 1.41 (s, 36H, *t*Bu); ^{13}C NMR ($CDCl_3$) δ (ppm): 160.1, 148.8, 148.7, 144.9, 143.4, 142.2, 141.9, 141.8, 141.6, 140.9, 140.5, 136.5, 131.8, 131.74, 131.71, 131.3, 131.1, 130.6, 129.3, 129.0, 120.8, 120.5, 119.4, 116.2, 109.4, 107.2, 103.9, 35.1, 31.80, 31.78 and 30.7; MALDI-TOF-MS m/z = 1782.73, calcd. for $C_{104}H_{114}N_8{}^{58}Ni_2{}^{192}Pt$ =1782.75 [M]$^+$; UV/Vis (CH_2Cl_2): λ_{max} (ε)= 400 (342000), 521 (32000) and 556 nm (16000 $M^{-1}cm^{-1}$).

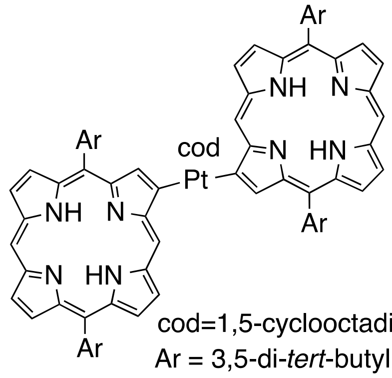

cod=1,5-cyclooctadiene
Ar = 3,5-di-*tert*-butylphenyl
2H

2H; 50.3 mg, 60% yield; ^{1}H NMR ($CDCl_3$, r.t.) δ (ppm): 11.15(s, 2H, por-*meso*), 10.06 (s, 2H, por-*meso*), 9.42 (s, 2H, por-β), 9.24 (d, J = 4.2 Hz, 2H, por-β), 9.21 (d, J = 4.8 Hz, 2H, por-β), 9.13 (d, J = 4.2 Hz, 2H, por-β), 8.99 (d, J = 4.8 Hz, 2H, por-β), 8.91 (d, J = 4.2 Hz, 2H, por-β), 8.82 (d, J = 4.8 Hz, 2H, por-β), 8.02 (m, 4H, aryl-*ortho*), 7.98 (m, 4H, aryl-*ortho*), 7.84 (m, 2H, aryl-*para*), 7.78 (m, 2H, aryl-*para*), 6.06 (m, 4H, cod), 3.23 (m, 4H, cod), 2.95 (m, 4H, cod), 1.53 (s, 36H, *t*Bu), 1.44 (s, 36H, *t*Bu), -3.19 (s, 2H, inner *N*H) and -3.39 (s, 2H, inner *N*H); ^{13}C NMR ($CDCl_3$) δ (ppm): 148.86, 148.81, 146.1, 143.8, 141.8, 141.3, 140.8, 139.9, 135.1, 133.2, 132.8, 132.3, 132.2, 131.8, 130.5, 130.1, 128.6, 128.3, 123.6, 120.8, 120.5, 120.2, 117.2, 107.9, 107.8, 107.7, 104.0, 35.12, 35.10, 31.84, 31.83 and 30.8; MALDI-TOF-MS m/z = 1671.20, calcd. for $C_{104}H_{118}N_8{}^{192}Pt$ =1670.91[M]$^+$; UV/Vis (CH_2Cl_2): λ_{max} (ε)= 407 (431000), 427 (242000), 512 (31000), 577 (9000) and 631 nm (6000 $M^{-1}cm^{-1}$).

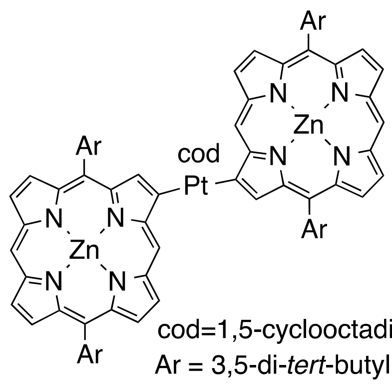

cod=1,5-cyclooctadiene
Ar = 3,5-di-*tert*-butylphenyl
2Zn

2Zn; 73.9 mg, 82% yield; ^{1}H NMR ($CDCl_3$, r.t.) δ (ppm): 11.11 (s, 2H, por-*meso*), 10.05 (s, 2H, por-*meso*), 9.44 (s, 2H, por-β), 9.27 (d, J = 4.2 Hz, 2H, por-β), 9.23 (d, J = 4.2 Hz, 2H, por-β), 9.21 (d, J = 4.8 Hz, 2H, por-β), 8.99 (m, 4H, por-β), 8.92 (d, J = 4.8 Hz, 2H, por-β), 7.99 (m, 4H, aryl-*ortho*), 7.98 (m, 4H, aryl-*ortho*), 7.88 (m, 2H, aryl-*para*), 7.77 (m, 2H, aryl-*para*), 6.10 (m, 4H, cod), 3.24 (m, 4H, cod), 2.96 (m, 4H, cod), 1.51 (s, 36H, *t*Bu), and 1.49 (s, 36H, *t*Bu); ^{13}C NMR ($CDCl_3$) δ (ppm): 160.7, 156.2, 152.7, 150.6, 149.0, 148.9, 148.8, 148.6, 148.42, 148.38, 142.4, 141.9, 135.7, 131.9, 131.8, 131.0, 130.8, 130.3, 130.2, 129.8, 121.1, 120.5, 120.2, 118.2, 110.8, 107.1, 105.0, 35.1, 35.0, 31.81, 31.77 and 30.7; MALDI-TOF-MS m/z = 1794.45, calcd. for $C_{104}H_{114}N_8{}^{64}Zn_2{}^{192}Pt$ =1794.73 [M]$^+$; UV/Vis (CH_2Cl_2): λ_{max} (ε)= 407 (507000), 424 (263000), 541 (45000) and 577 nm (13000 $M^{-1}cm^{-1}$); Fluorescence (CH_2Cl_2, λ_{ex} = 410 nm): λ_{max} = 589 and 632 nm, Φ_F < 0.001.

2.4 General procedure for the synthesis of 3M.

A flask containing **2M** (0.050 mmol), triphenylphosphine (131.0 mg, 0.50 mmol) was purged with argon, charged with anhydrous toluene (10 mL) and stirred at reflux for 4 hours. After cooled down to room temperature, toluene was removed under vacuum. The residue was dissolved in $CHCl_3$ (20 mL) and washed with brine (20 mL) for three times. After dried over anhydrous sodium sulfate, the organic layer was evaporated to dryness under vacuum. The mixture was purified by column chromatography on silica using CH_2Cl_2/hexane (*v/v*=1/1) as an eluent to give **3M**.

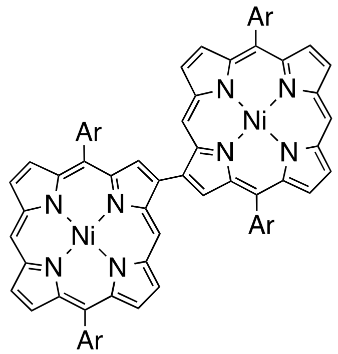

Ar = 3,5-di-*tert*-butylphenyl

3Ni

3Ni; 60.1 mg, 81% yield; ^{1}H NMR ($CDCl_3$, r.t.) δ (ppm): 10.24 (s, 2H, por-*meso*), 9.97 (s, 2H, por-*meso*), 9.49 (s, 2H, por-β), 9.25 (d, J = 4.2 Hz, 2H, por-β), 9.22 (d, J = 4.2 Hz, 2H, por-β), 9.11 (d, J = 4.2 Hz, 2H, por-β), 9.01 (d, J = 4.2 Hz, 2H, por-β), 8.90 (d, J = 4.8 Hz, 2H, por-β), 8.89 (d, J = 4.8 Hz, 2H, por-β), 8.14 (d, J = 1.8 Hz, 4H, aryl-*ortho*), 7.93 (d, J = 1.8 Hz, 4H, aryl-*ortho*), 7.75 (t, J = 1.8 Hz, 2H, aryl-*para*), 7.70 (t, J = 1.8 Hz, 2H, aryl-*para*), 1.50 (s, 36H, *t*Bu), and 1.49 (s, 36H, *t*Bu); ^{13}C NMR ($CDCl_3$) δ (ppm): 149.1, 149.0, 143.31, 143.27, 143.24, 143.1, 142.9, 142.8, 142.3, 142.0, 140.1, 139.9, 139.4, 134.0, 132.9, 132.8, 132.6, 132.2, 132.1, 132.0, 129.1, 129.0, 128.2, 121.23, 121.18, 119.9, 119.8, 105.5, 104.9, 35.0, 31.8 and 31.7; MALDI-TOF-MS *m/z* = 1482.79, calcd. for $C_{96}H_{102}N_8{}^{58}Ni_2$ =1482.69 $[M]^+$; UV/Vis (CH_2Cl_2): λ_{max} (ε)= 408 (223000), 523 (35000) and 568 nm (26000 $M^{-1}cm^{-1}$).

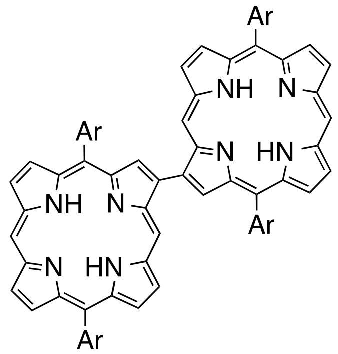

Ar = 3,5-di-*tert*-butylphenyl

3H

3H; 52.1 mg, 76% yield; ^{1}H NMR ($CDCl_3$, r.t.) δ (ppm): 10.75(s, 2H, por-*meso*), 10.38 (s, 2H, por-*meso*), 9.77 (s, 2H, por-β), 9.52 (d, J = 4.8 Hz, 2H, por-β), 9.42 (d, J = 4.8 Hz, 2H, por-β), 9.29 (d, J = 4.2 Hz, 2H, por-β), 9.14 (d, J = 4.8 Hz, 2H, por-β), 9.11 (d, J = 4.8 Hz, 2H, por-β), 9.07 (d, J = 4.8 Hz, 2H, por-β), 8.42 (d, J = 1.8 Hz, 4H, aryl-*ortho*), 8.15 (d, J = 1.8 Hz, 4H, aryl-*ortho*), 7.82 (t, J = 1.8 Hz, 2H, aryl-*para*), 7.79 (t, J = 1.8 Hz, 2H, aryl-*para*), 1.57 (s, 36H, *t*Bu), 1.56 (s, 36H, *t*Bu), -2.65 (s, 2H, inner *N*H) and -2.69 (s, 2H, inner *N*H); ^{13}C NMR ($CDCl_3$) δ (ppm): 150.7, 149.2, 149.1, 148.4, 148.3, 144.6, 142.5, 140.9, 140.6, 140.3, 134.3, 132.8, 132.6, 130.6, 130.4, 130.2, 130.1, 129.9, 121.2, 121.1, 120.8, 120.7, 105.5, 105.1, 35.11, 35.09, 31.83 and 31.75; MALDI-TOF-MS *m/z* = 1370.96, calcd. for $C_{96}H_{106}N_8$ =1370.85 [*M*]$^+$; UV/Vis (CH_2Cl_2): λ_{max} (ε)= 410 (312000), 511 (44000), 544 (14000), 583 (16000) and 637 nm (3000 $M^{-1}cm^{-1}$).

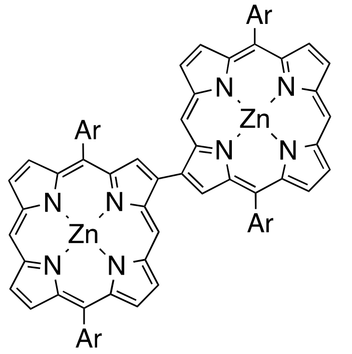

Ar = 3,5-di-*tert*-butylphenyl

3Zn

3Zn; 58.4 mg, 78% yield; ^{1}H NMR ($CDCl_3$, r.t.) δ (ppm): 10.89 (s, 2H, por-*meso*), 10.41 (s, 2H, por-*meso*), 9.90 (s, 2H, por-β), 9.54 (d, J = 4.8 Hz, 2H, por-β), 9.51 (d, J = 4.8 Hz, 2H, por-β), 9.32 (d, J = 4.2 Hz, 2H, por-β), 9.24 (d, J = 4.2 Hz, 2H, por-β), 9.23 (d, J = 4.2 Hz, 2H, por-β), 9.16 (d, J = 4.2 Hz, 2H, por-β), 8.42 (d, J = 1.2 Hz, 4H, aryl-*ortho*), 8.16 (d, J = 1.2 Hz, 4H, aryl-*ortho*), 7.84 (t, J = 1.2 Hz, 2H, aryl-*para*), 7.78 (t, J = 1.2 Hz, 2H, aryl-*para*), 1.58 (s, 36H, *t*Bu), and 1.57 (s, 36H, *t*Bu); ^{13}C NMR ($CDCl_3$) δ (ppm): 150.9, 150.6, 150.5, 149.84, 149.78, 149.6, 149.3, 148.80, 148.75, 141.8, 141.5, 140.0, 134.7, 133.1, 133.0, 132.7, 132.0, 131.8, 131.7, 129.92, 129.88, 121.8, 121.0, 120.9, 106.3, 106.2, 35.12, 35.10, 31.9 and 31.8; MALDI-TOF-MS *m/z* = 1494.77, calcd. for $C_{96}H_{102}N_8{}^{64}Zn_2$ =1494.68 [*M*]$^+$; UV/Vis (CH_2Cl_2): λ_{max} (ε) = 411 (294000), 544 (44000) and 584 nm (19000 $M^{-1}cm^{-1}$); Fluorescence (CH_2Cl_2, λ_{ex} = 411 nm): λ_{max} = 590 and 640 nm, Φ_F = 0.049.

2.5 General procedure for the synthesis of 5Ni and 5Zn.

4M (0.10 mmol), Pt(cod)Cl_2 (37.4 mg, 0.10 mmol) and CsF (182.0 mg, 1.20 mmol) in 1,4-dioxane (20 mL) were stirred at reflux for 12 h under inert atmosphere. Then the mixture was cooled down to room temperature and 1,4-dioxane was removed under vacuum. The residue was dissolved in small amount of CH_2Cl_2 and was filtered. Then CH_2Cl_2 was removed and the crude mixture was purified by recrystallization from CH_2Cl_2/methanol twice to give pure **5Ni** and **5Zn**.

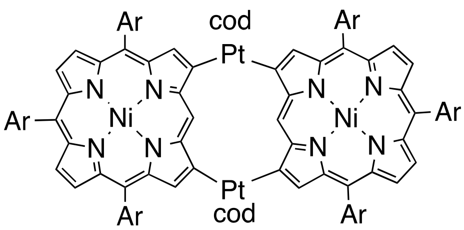

cod=1,5-cyclooctadiene

Ar = 3,5-di-*tert*-butylphenyl

5Ni

5Ni: 104.0 mg, 84% yield; ^{1}H NMR ($CDCl_3$, –50 ºC) δ (ppm): 11.86 (s, 2H, por-*meso*), 8.76 (s, 4H, por-β), 8.69 (d, J = 4.8 Hz, 4H, por-β), 8.65 (d, J = 4.8 Hz, 4H, por-β), 8.62 (m, 4H, aryl-*ortho*), 8.49

(m, 2H, aryl-*para*), 7.62 (m, 4H, aryl-*ortho*), 7.59 (m, 2H, aryl-*para*), 7.14 (m, 4H, aryl-*ortho*), 7.13 (m, 2H, aryl-*para*), 5.73 (m, 8H, cod), 2.96 (m, 8H, cod), 2.76 (m, 8H, cod), 1.65 (s, 36H, *t*Bu), 1.53 (s, 18H, *t*Bu), 1.27 (s, 18H, *t*Bu), and 1.10 (s, 36H, *t*Bu); ^{13}C NMR ($CDCl_3$) δ (ppm): 158.9, 148.5, 148.0, 144.4, 142.3, 140.7, 140.5, 135.5, 130.7, 130.1, 128.5, 120.5, 120.1, 118.6, 116.4, 108.4, 104.1, 35.05, 34.97, 31.7, 30.6 and 30.3; MALDI-TOF-MS *m/z* = 2356.95, calcd. for $C_{132}H_{152}N_8{}^{58}Ni_2{}^{192}Pt_2$ =2357.02 [*M*-COD]$^+$; UV/Vis (CH_2Cl_2): λ_{max} (ε)= 412 (333000) and 530 nm (43000 $M^{-1}cm^{-1}$).

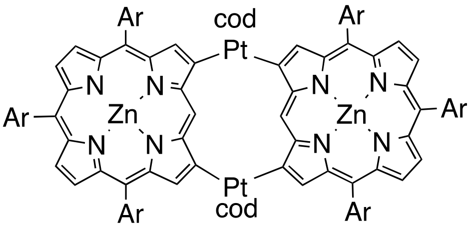

cod=1,5-cyclooctadiene
Ar = 3,5-di-*tert*-butylphenyl
5Zn

5Zn; 87.0 mg, 70% yield; ^{1}H NMR ($CDCl_3$, r.t.) δ (ppm): 12.89 (s, 2H, por-*meso*), 8.97 (s, 4H, por-β), 8.72 (d, J = 4.8 Hz, 4H, por-β), 8.70 (d, J = 4.8 Hz, 4H, por-β), 8.25 (t, J = 1.8 Hz, 4H, aryl-*ortho*), 8.03 (t, J = 1.8 Hz, 2H, aryl-*para*), 7.81 (t, J = 1.8 Hz, 4H, aryl-*ortho*), 7.78 (t, J = 1.8 Hz, 4H, aryl-*ortho*), 7.70 (t, J = 1.8 Hz, 2H, aryl-*para*), 7.61 (t, J = 1.8 Hz, 2H, aryl-*para*), 6.26 (m, 8H, cod), 3.39 (m, 4H, cod), 3.16 (m, 4H, cod), 3.07 (m, 4H, cod), 2.98 (m, 4H, cod), 1.67 (s, 36H, *t*Bu), 1.42 (s, 36H, *t*Bu), 1.41 (s, 18H, *t*Bu), and 1.36 (s, 18H, *t*Bu); UV/Vis (CH_2Cl_2): MALDI-TOF-MS *m/z* = 2371.00, calcd. for $C_{132}H_{152}N_8{}^{64}Zn_2Pt_2$ =2371.00 [*M*-COD]$^+$; UV/Vis (CH_2Cl_2): λ_{max} (ε)= 421 (219000) and 548 nm (32000 $M^{-1}cm^{-1}$); Fluorescence (CH_2Cl_2, λ_{ex} = 420s nm): λ_{max} = 599 and 643 nm, Φ_F < 0.001.

2.6 Synthesis of 6Ni.

A flask containing **5Ni** (24.7 mg, 0.010 mmol), triphenylphosphine (52.4 mg, 0.20 mmol) was purged with argon, charged with anhydrous toluene (10 mL) and stirred at reflux for 3 h. After cooled down to room temperature, toluene was removed under vacuum. The residue was dissolved in $CHCl_3$ (10 mL) and washed with brine (10 mL) for three times. After dried over anhydrous sodium sulfate, the organic layer was evaporated to dryness under vacuum. The mixture was purified by a silica gel column using CH_2Cl_2/hexane (*v/v*=1/1) as the eluent to give **6Ni**.

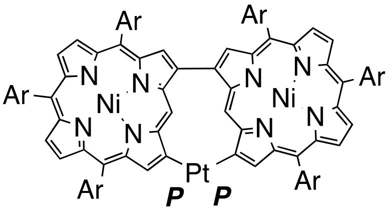

P = triphenylphosphine
Ar = 3,5-di-*tert*-butylphenyl
6Ni

6Ni; 20.1mg, 78% yield; ^{1}H NMR ($CDCl_3$, –60 ºC) δ (ppm): 11.79 (s, 2H, por-*meso*), 9.00 (s, 2H, por-β), 8.93 (d, J = 4.2 Hz, 2H, por-β), 8.87 (d, J = 4.2 Hz, 2H, por-β), 8.76 (d, J = 4.2 Hz, 2H, por-β), 8.72 (s, 2H, aryl-*ortho*), 8.57 (s, 2H, aryl-*ortho*), 8.55 (d, J = 4.2 Hz, 2H, por-β), 8.39 (s, 2H, aryl-*ortho*), 8.01 (s, 2H, por-*β*), 7.71 (s, 2H, aryl-*para*), 7.69 (s, 2H, aryl-*para*), 7.66 (s, 2H, aryl-*para*), 7.34 (s, 2H, aryl-*ortho*), 7.19 (s, 2H, aryl-*ortho*), 6.98 (m, 12H, phenyl), 6.95 (s, 2H, aryl-*ortho*), 6.51 (m, 6H, phenyl), 6.35 (m, 12H, phenyl), 1.76 (s, 18H, *t*Bu), 1.66 (s, 18H, *t*Bu), 1.63 (s, 18H, *t*Bu), 1.39 (s, 18H, *t*Bu), 1.31 (s, 18H, *t*Bu), and 1.29 (s, 18H, *t*Bu); ^{13}C NMR ($CDCl_3$) δ (ppm): 164.4, 151.3, 148.8, 148.7, 148.4, 145.5, 143.6, 143.3, 142.6, 141.4, 141.3, 140.5, 140.4, 140.34, 140.29, 138.3, 134.3, 133.3, 131.3, 131.2, 131.05, 130.98, 130.86, 130.7, 129.1, 128.9, 128.5, 128.2, 127.0, 120.71, 120.67, 120.1, 119.3, 118.3, 115.5, 108.5, 35.0, 31.9, 31.8 and 31.7; MALDI-TOF-MS *m/z* = 2579.21, calcd. for $C_{160}H_{170}N_8{}^{58}Ni_2P_2{}^{192}Pt$ =2579.14 $[M]^+$; UV/Vis (CH_2Cl_2): λ_{max} (ε)= 421 (235000), 538 (34000) and 604 nm (27000 $M^{-1}cm^{-1}$).

3. NMR Spectra

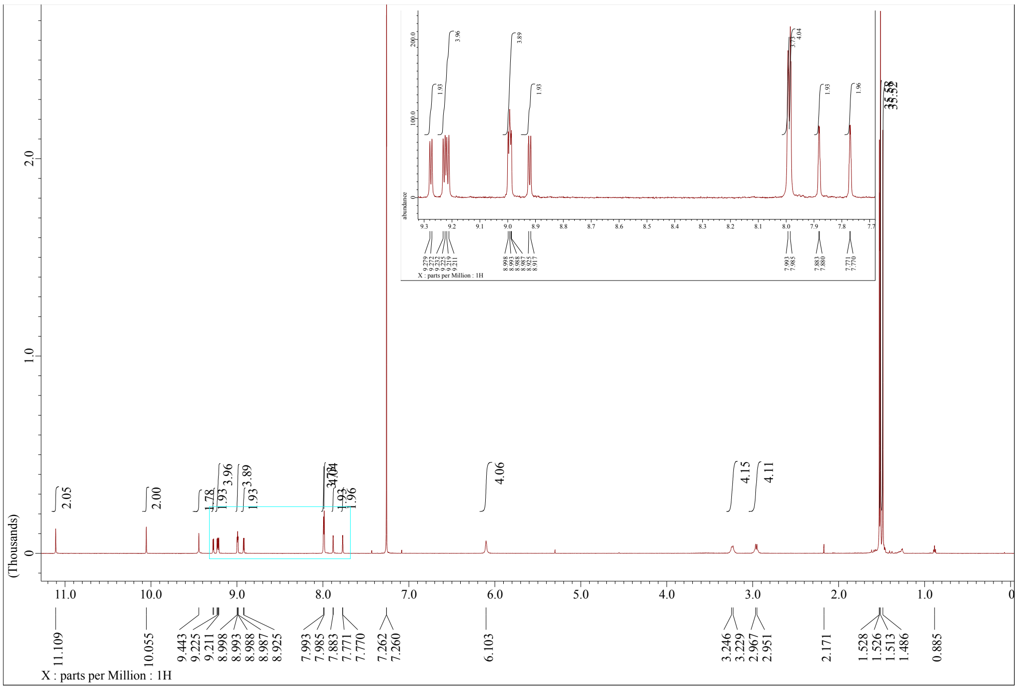

Figure S3-1. ^{1}H NMR spectrum of **2Zn** in $CDCl_3$ at room temperature.

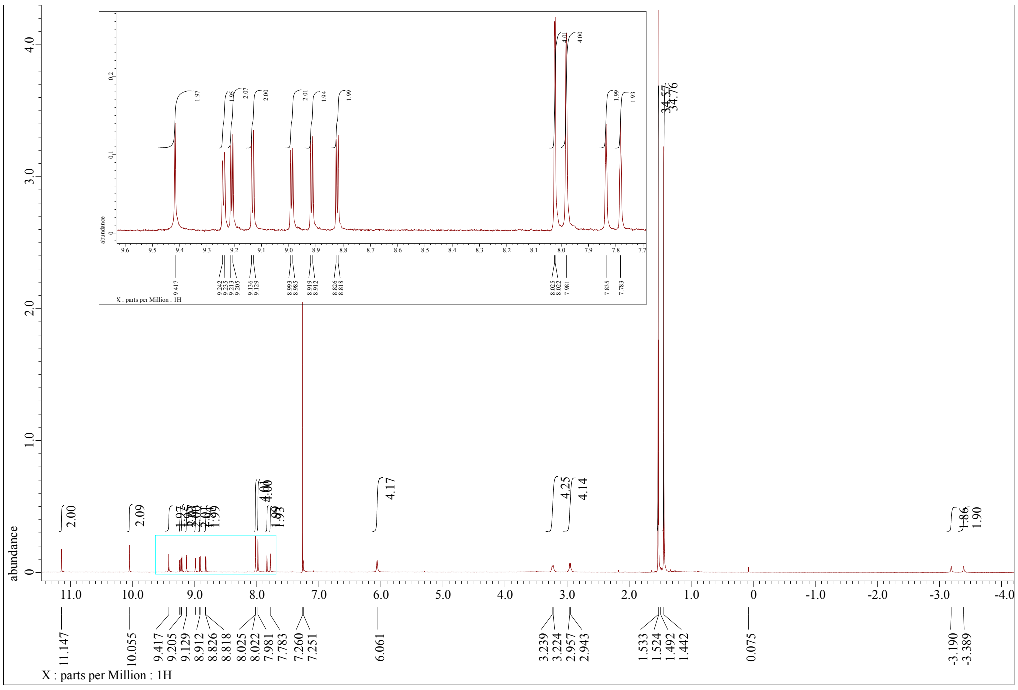

Figure S3-2. ^{1}H NMR spectrum of **2H** in $CDCl_3$ at room temperature.

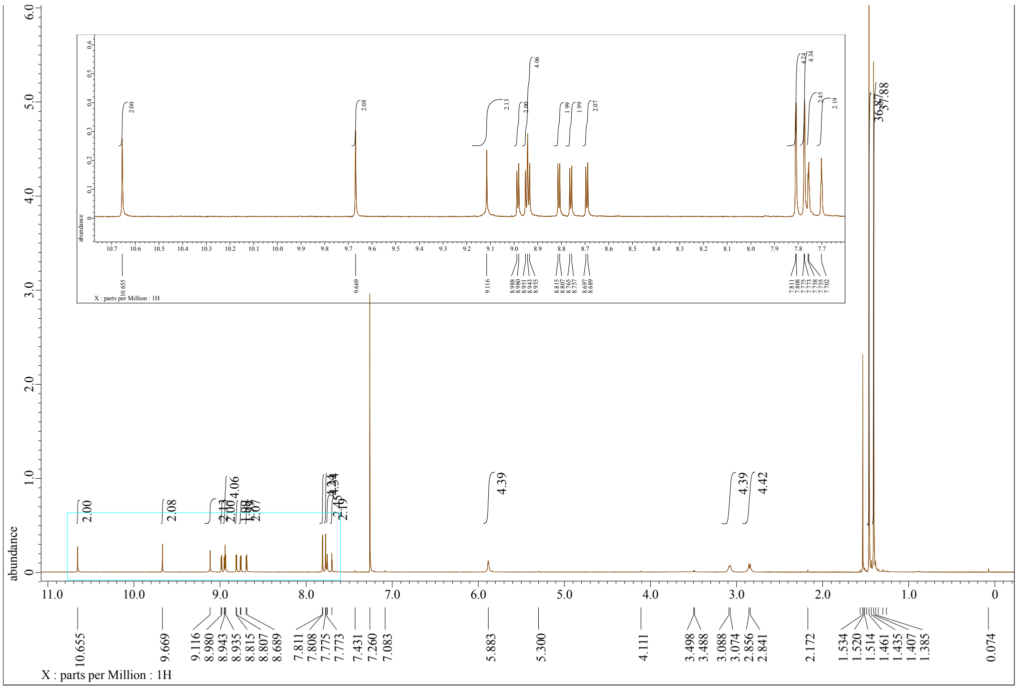

Figure S3-3. ^{1}H NMR spectrum of **2Ni** in $CDCl_3$ at room temperature.

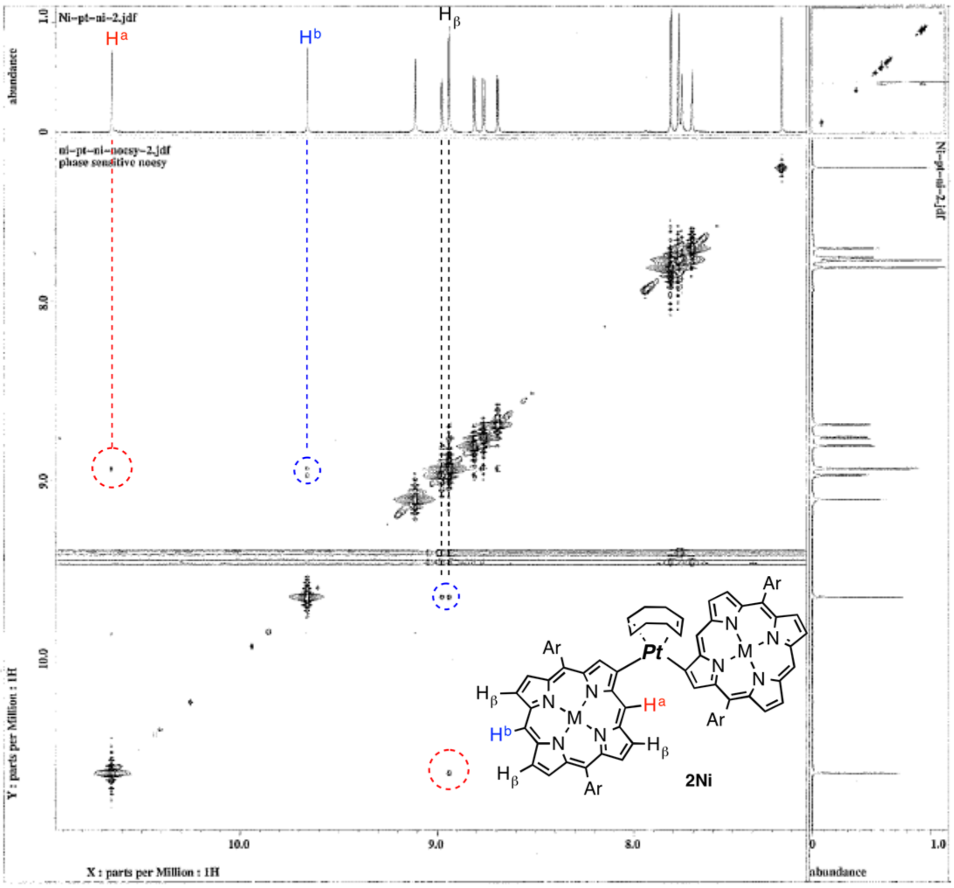

Figure S3-4. ^{1}H-^{1}H NOESY chart of **2Ni** measured in $CDCl_3$ at room temperature.

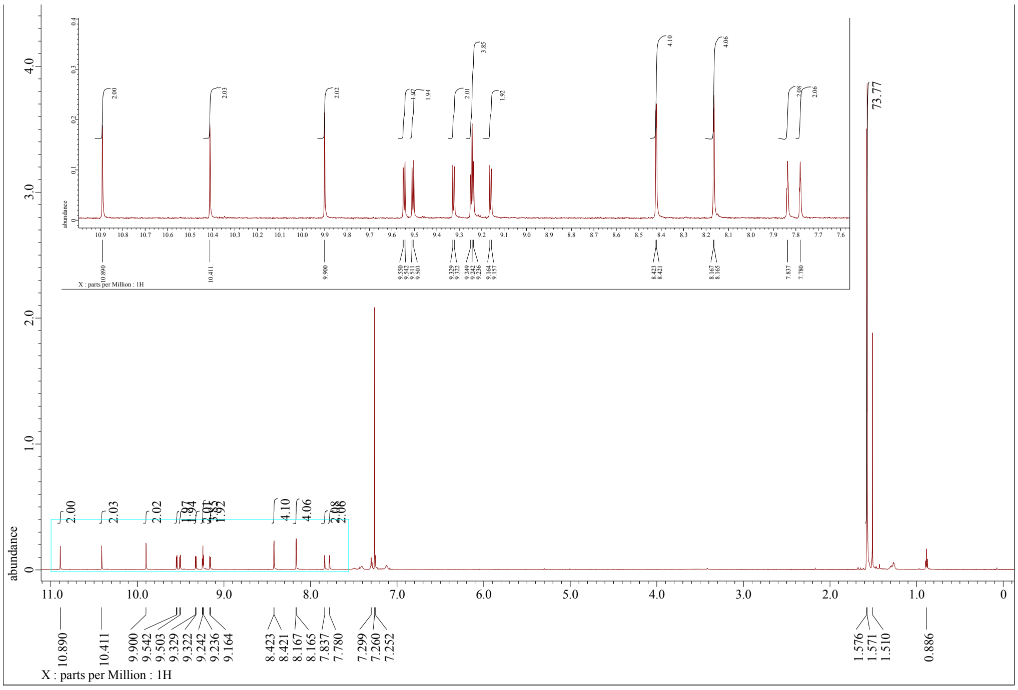

Figure S3-5. ^{1}H NMR spectrum of **3Zn** in $CDCl_3$ at room temperature.

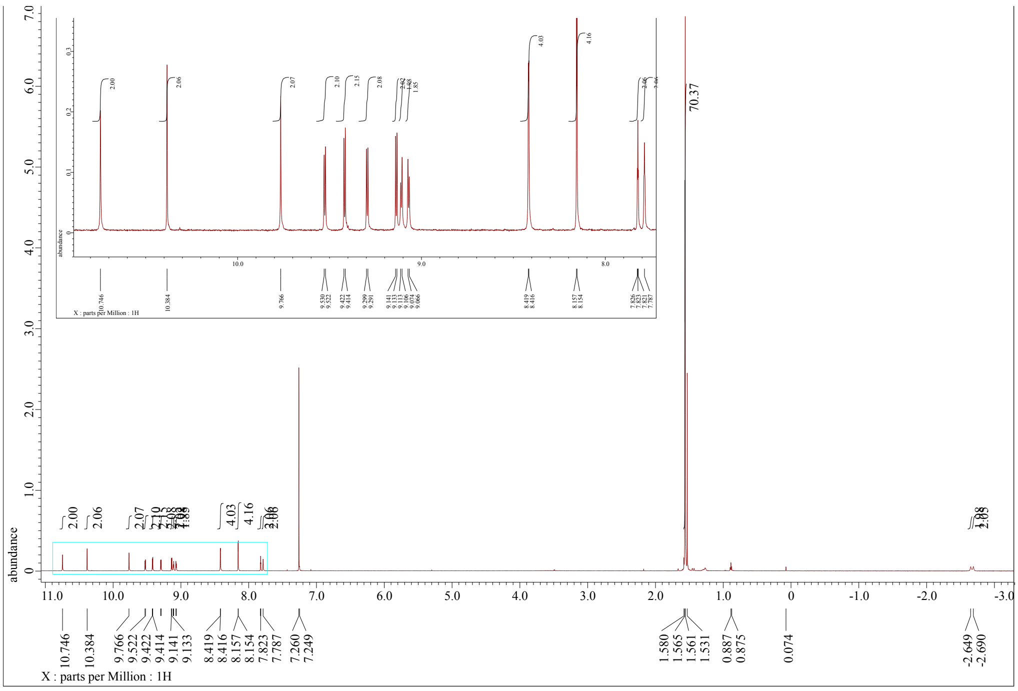

Figure S3-6. ^{1}H NMR spectrum of **3H** in $CDCl_3$ at room temperature.

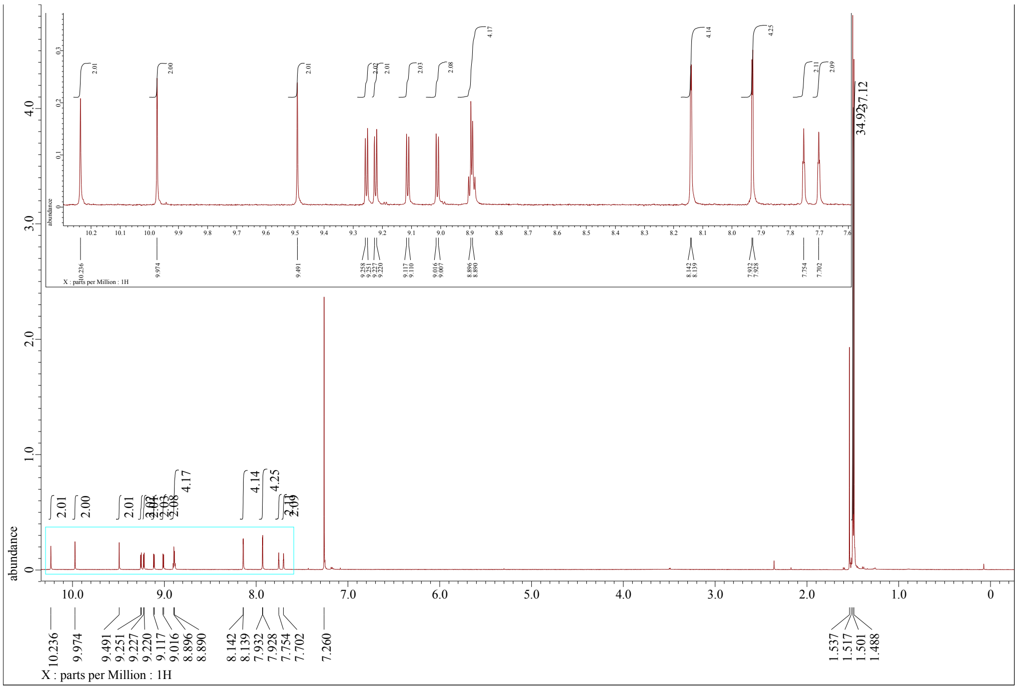

Figure S3-7. ^{1}H NMR spectrum of **3Ni** in $CDCl_3$ at room temperature.

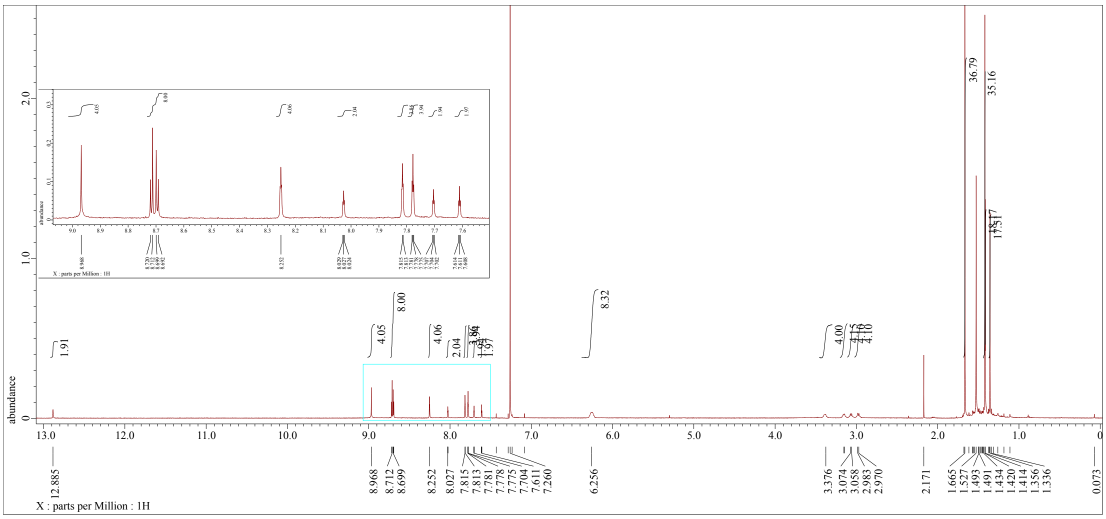

Figure S3-8. ^{1}H NMR spectrum of **5Zn** in $CDCl_3$ at room temperature.

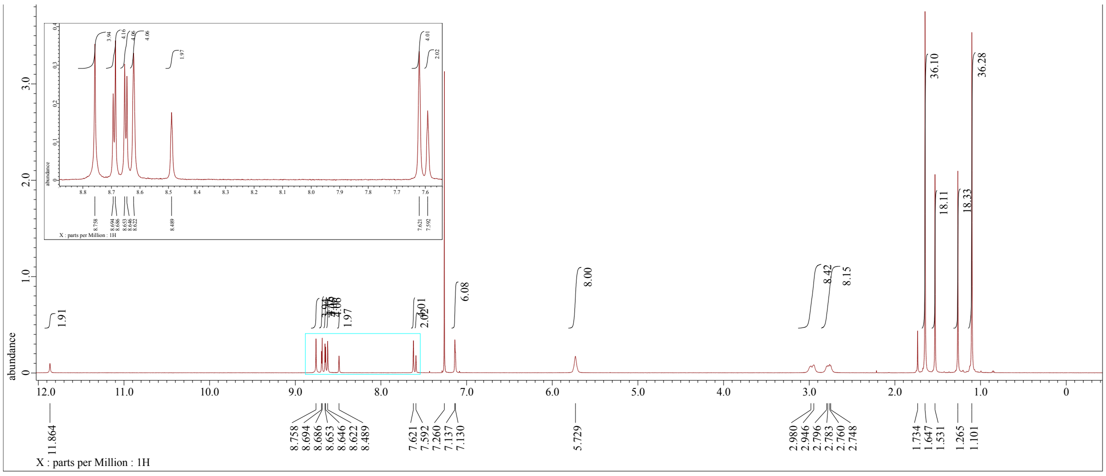

Figure S3-9. ^{1}H NMR spectrum of **5Ni** in $CDCl_3$ at –50 °C.

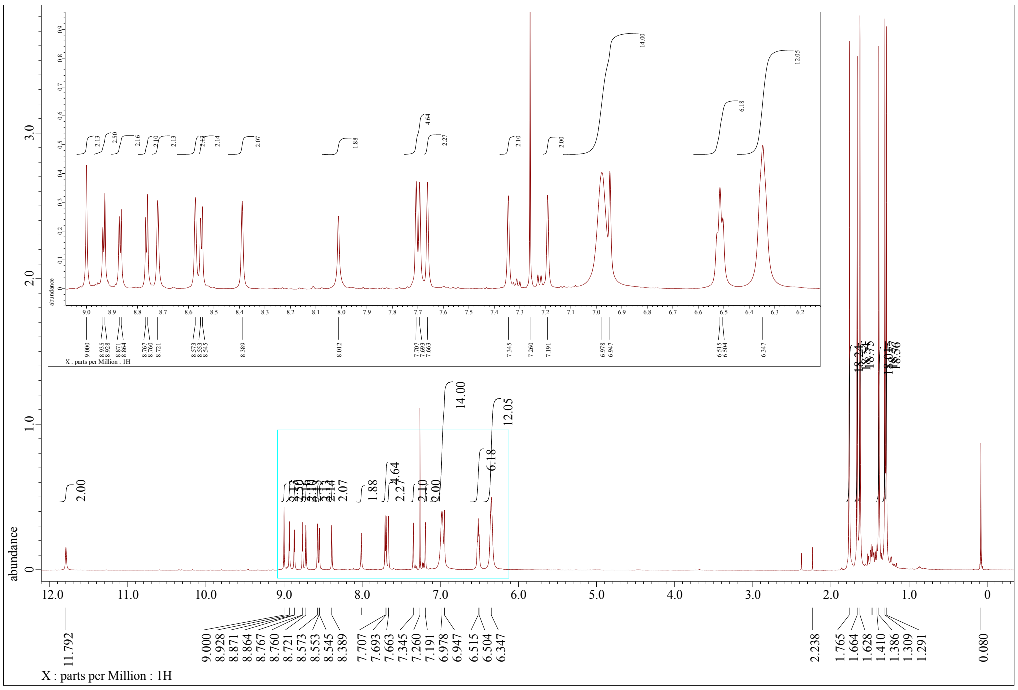

Figure S3-10. ^{1}H NMR spectrum of **6Ni** in $CDCl_3$ at –60 °C.

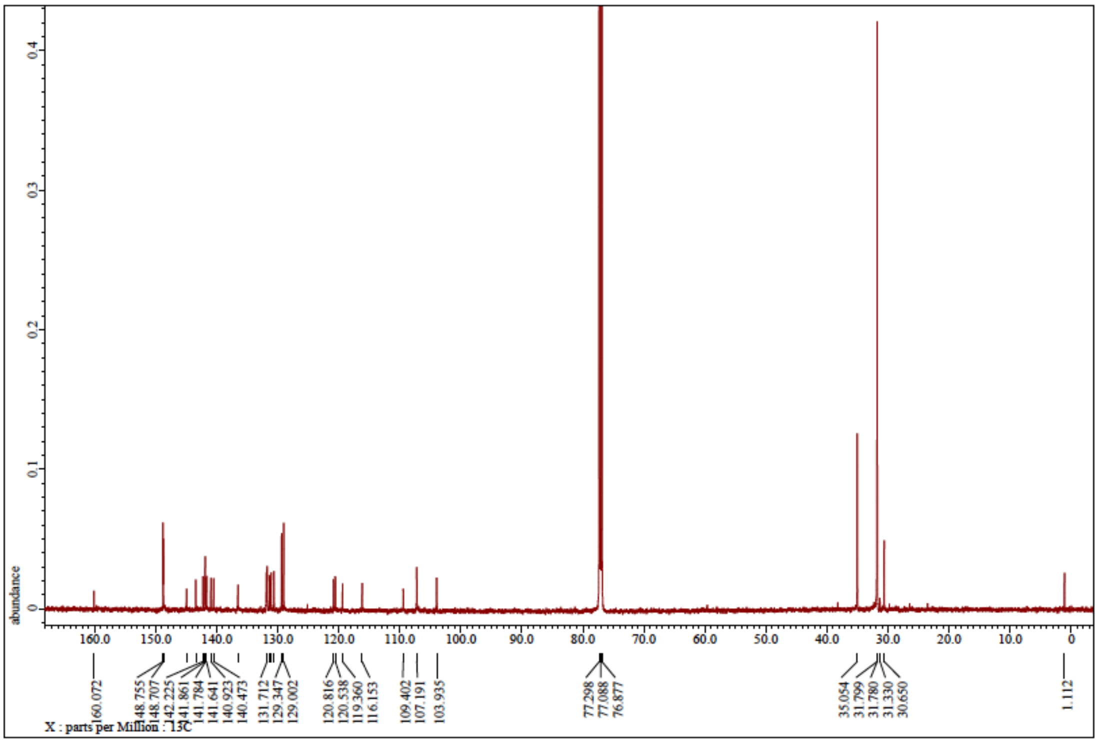

Figure S3-11. ^{13}C NMR spectrum of **2Ni** in $CDCl_3$ at room temperature.

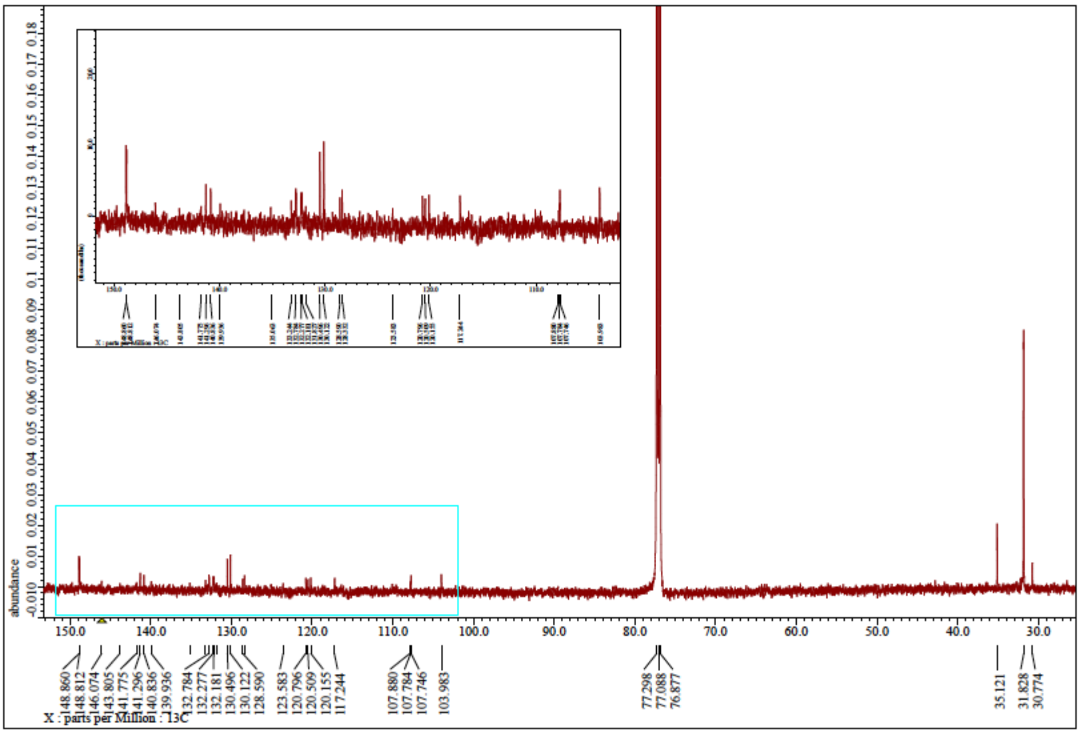

Figure S3-12. ^{13}C NMR spectrum of **2H** in $CDCl_3$ at room temperature.

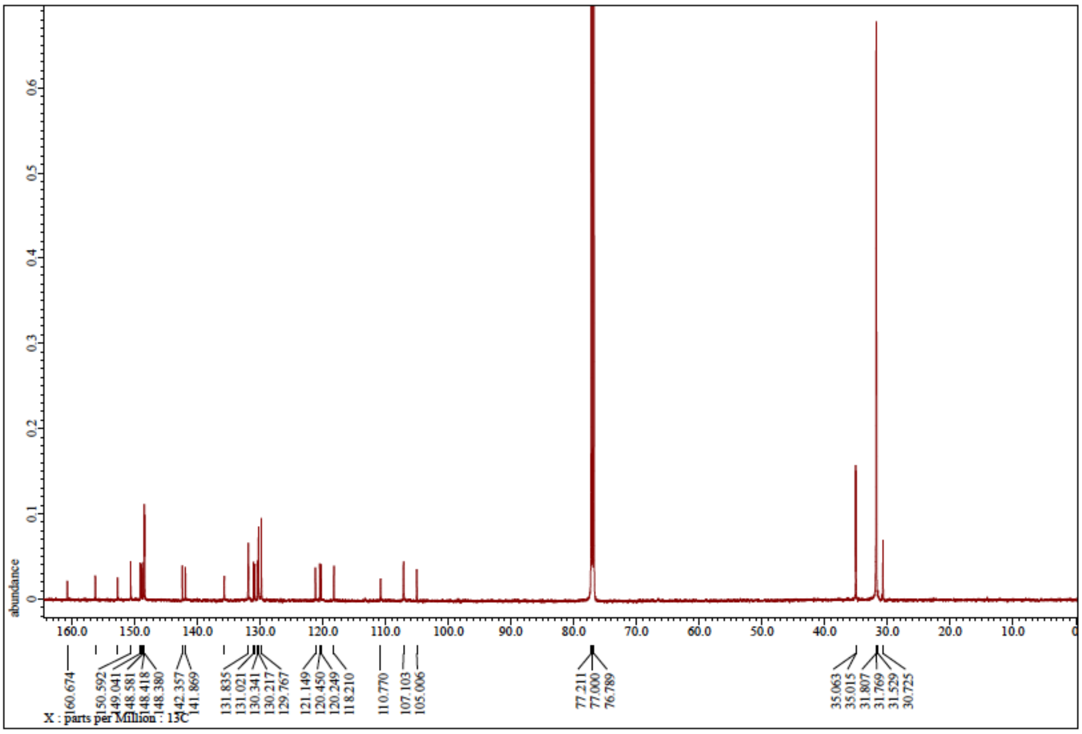

Figure S3-13. ^{13}C NMR spectrum of **2Zn** in $CDCl_3$ at room temperature.

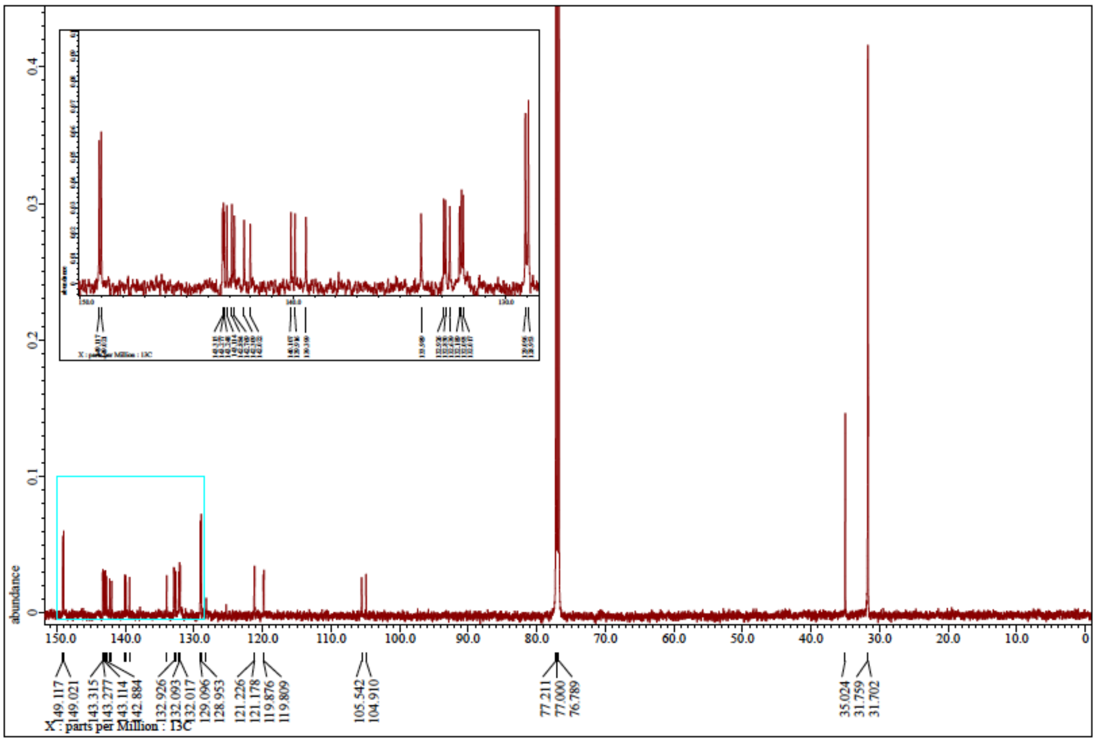

Figure S3-14. ^{13}C NMR spectrum of **3Ni** in $CDCl_3$ at room temperature.

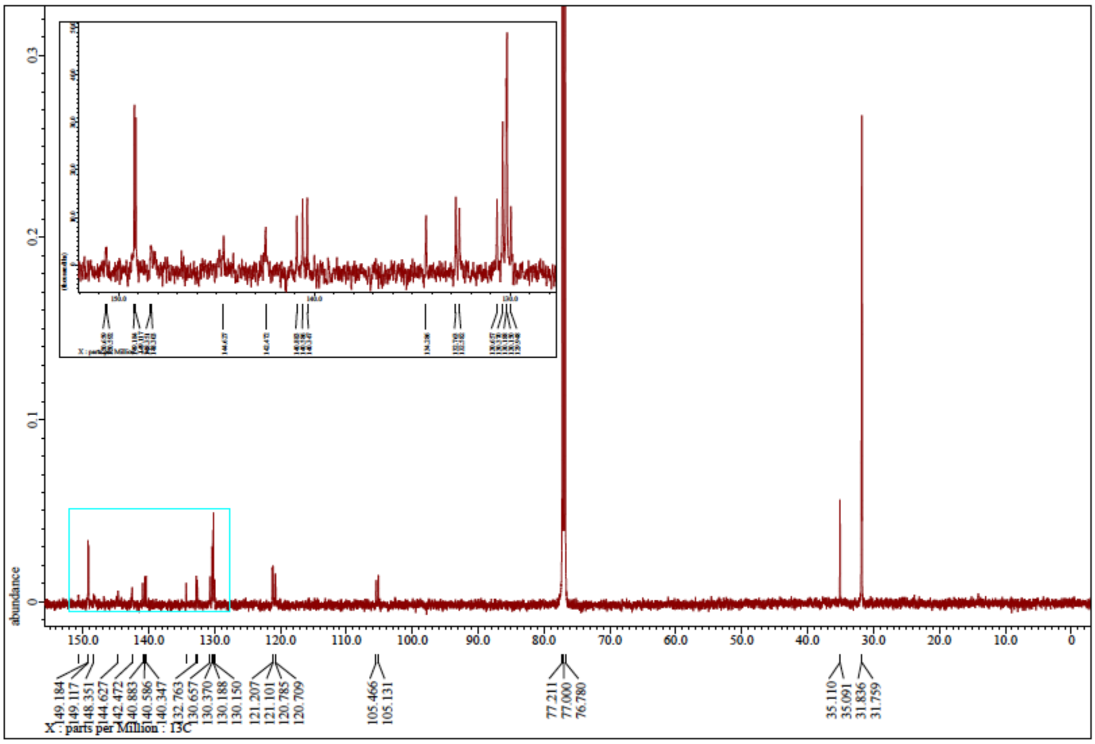

Figure S3-15. ^{13}C NMR spectrum of **3H** in $CDCl_3$ at room temperature.

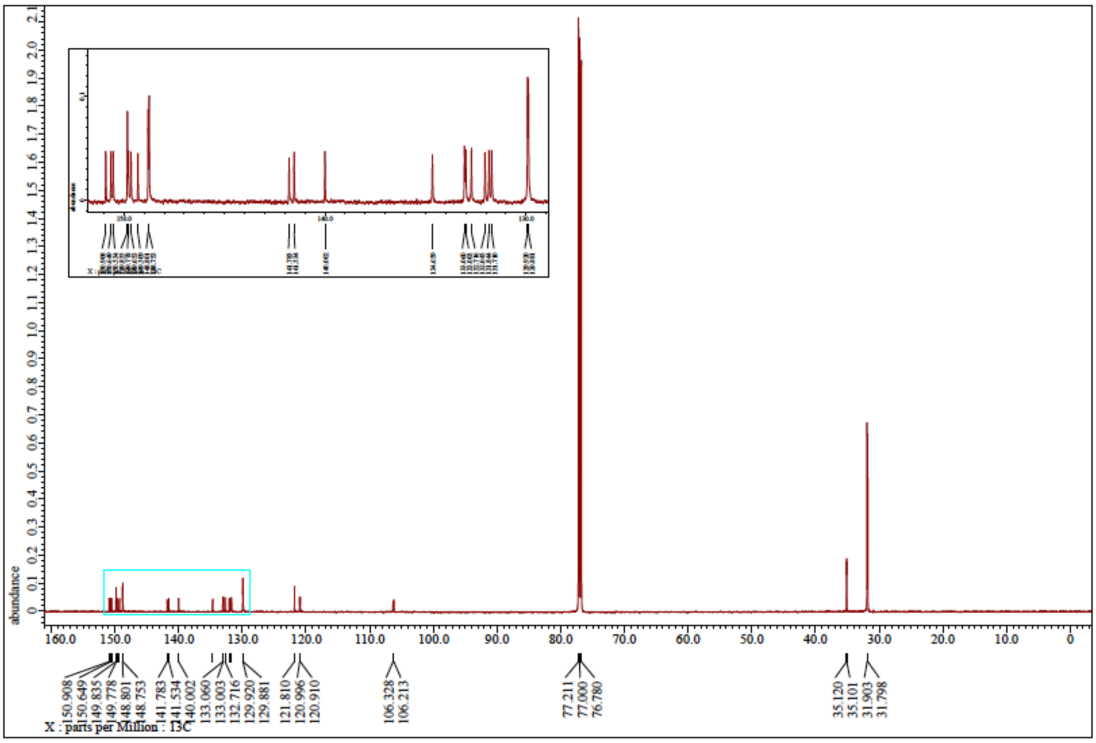

Figure S3-16. ^{13}C NMR spectrum of **3Zn** in $CDCl_3$ at room temperature.

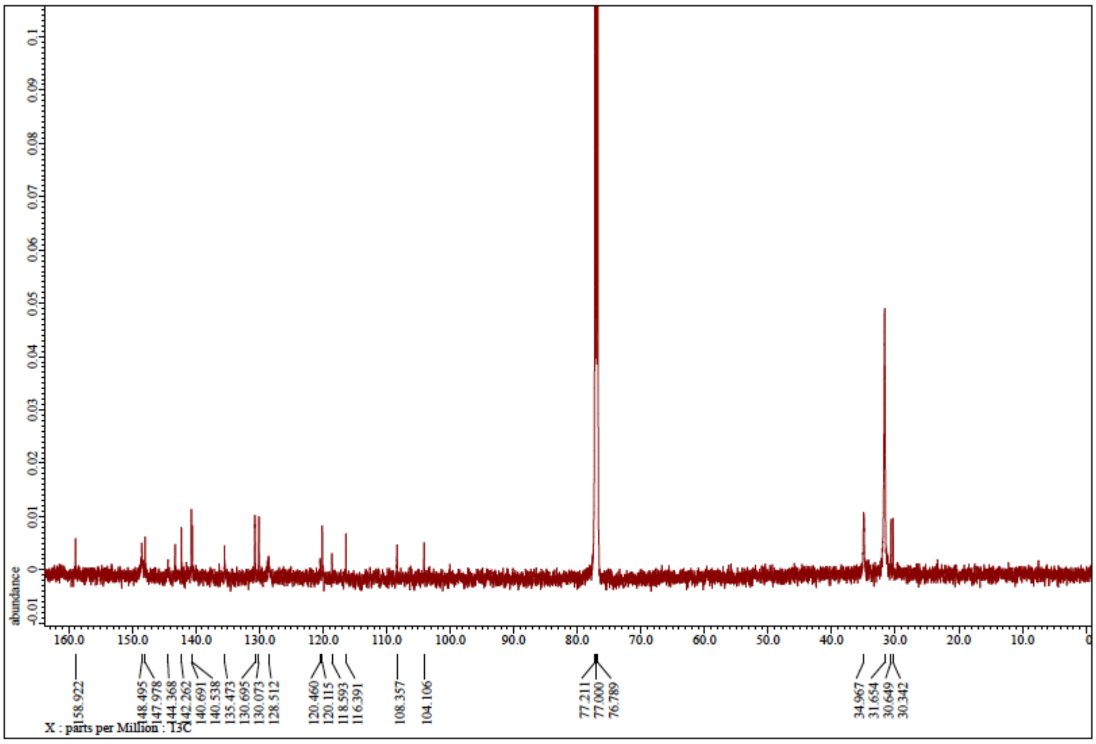

Figure S3-17. ^{13}C NMR spectrum of **5Ni** in $CDCl_3$ at room temperature.

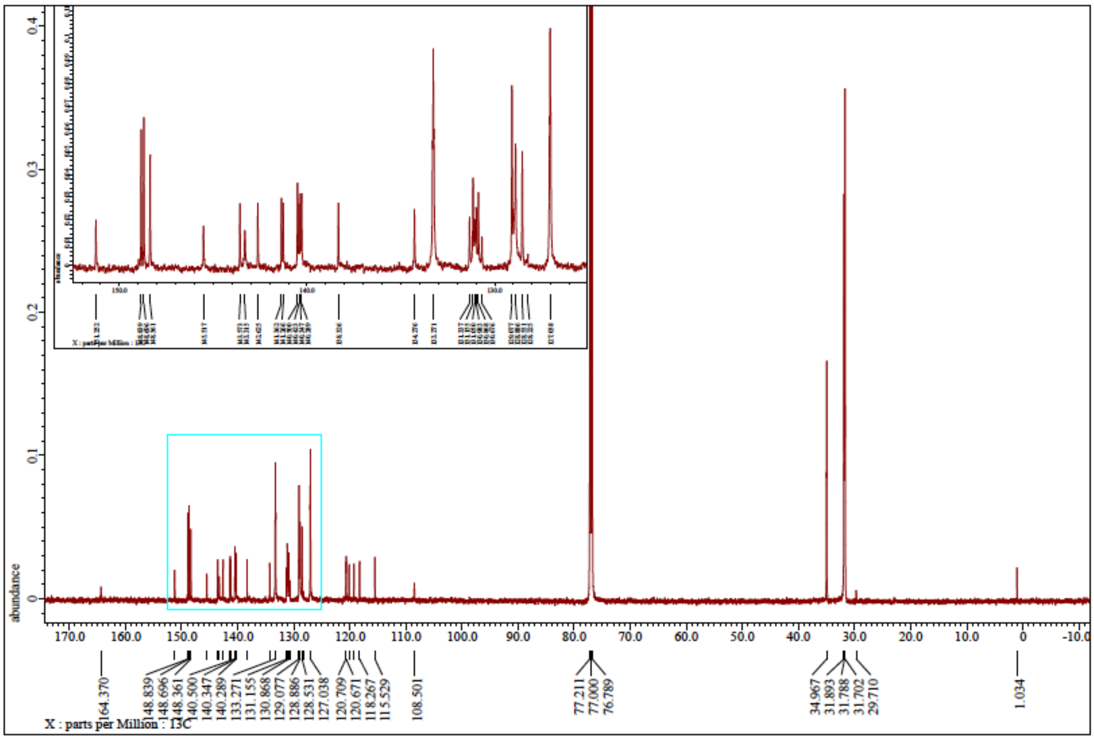

Figure S3-18. ^{13}C NMR spectrum of **6Ni** in $CDCl_3$ at room temperature.

4. Mass Spectra

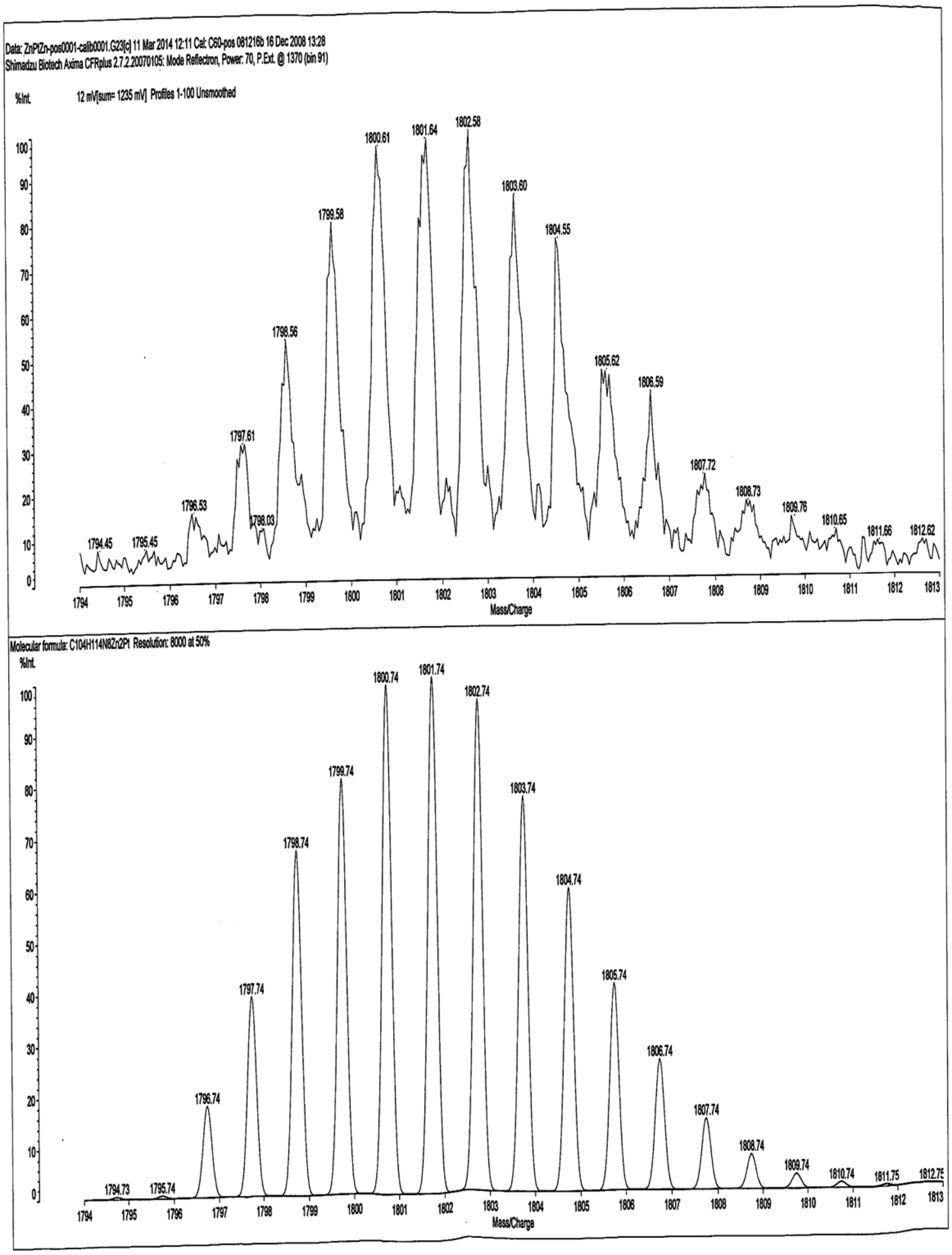

Figure S4-1. Simulated (bottom) and observed (top) MALDI-TOF-MS of **2Zn**.

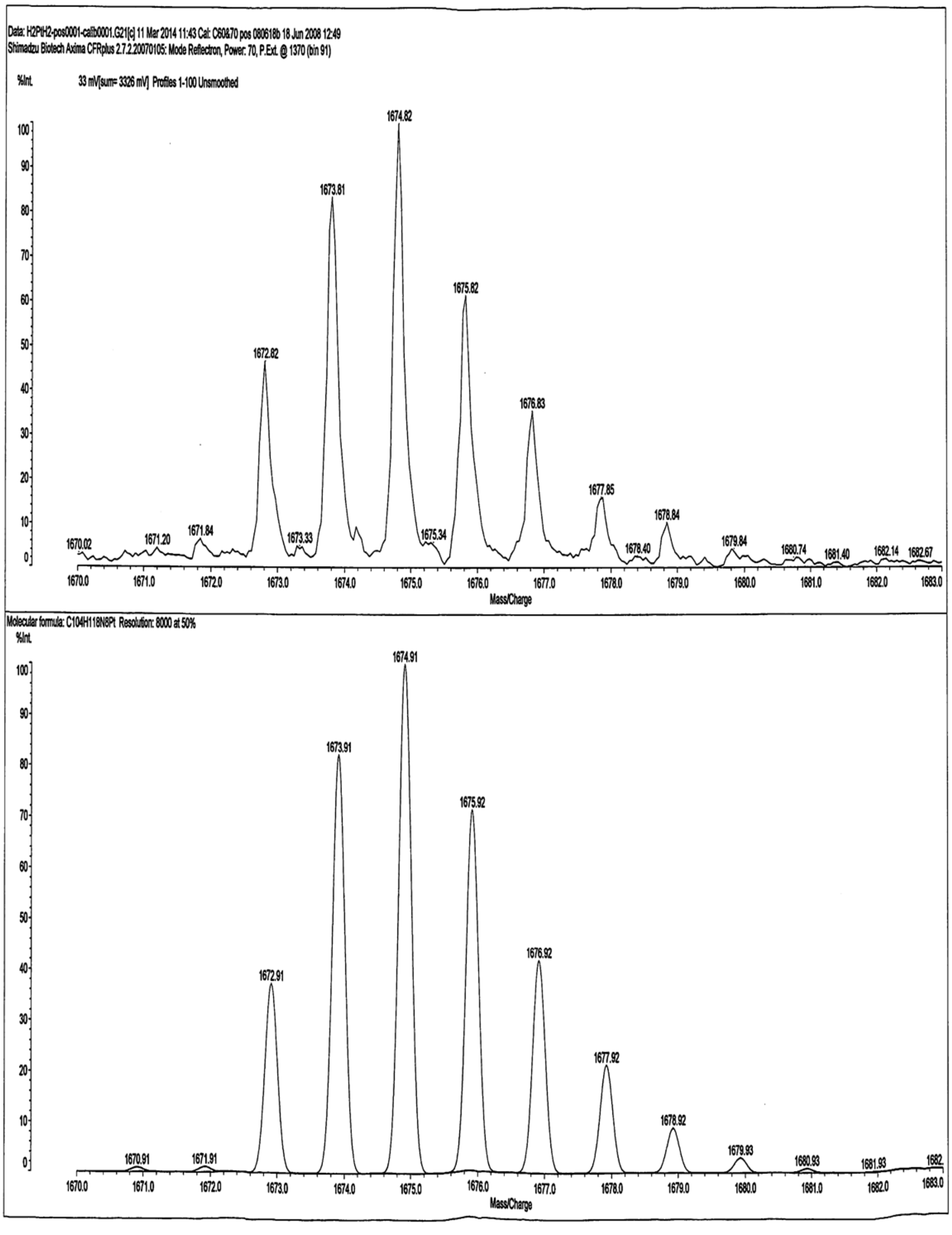

Figure S4-2. Simulated (bottom) and observed (top) MALDI-TOF-MS of **2H**.

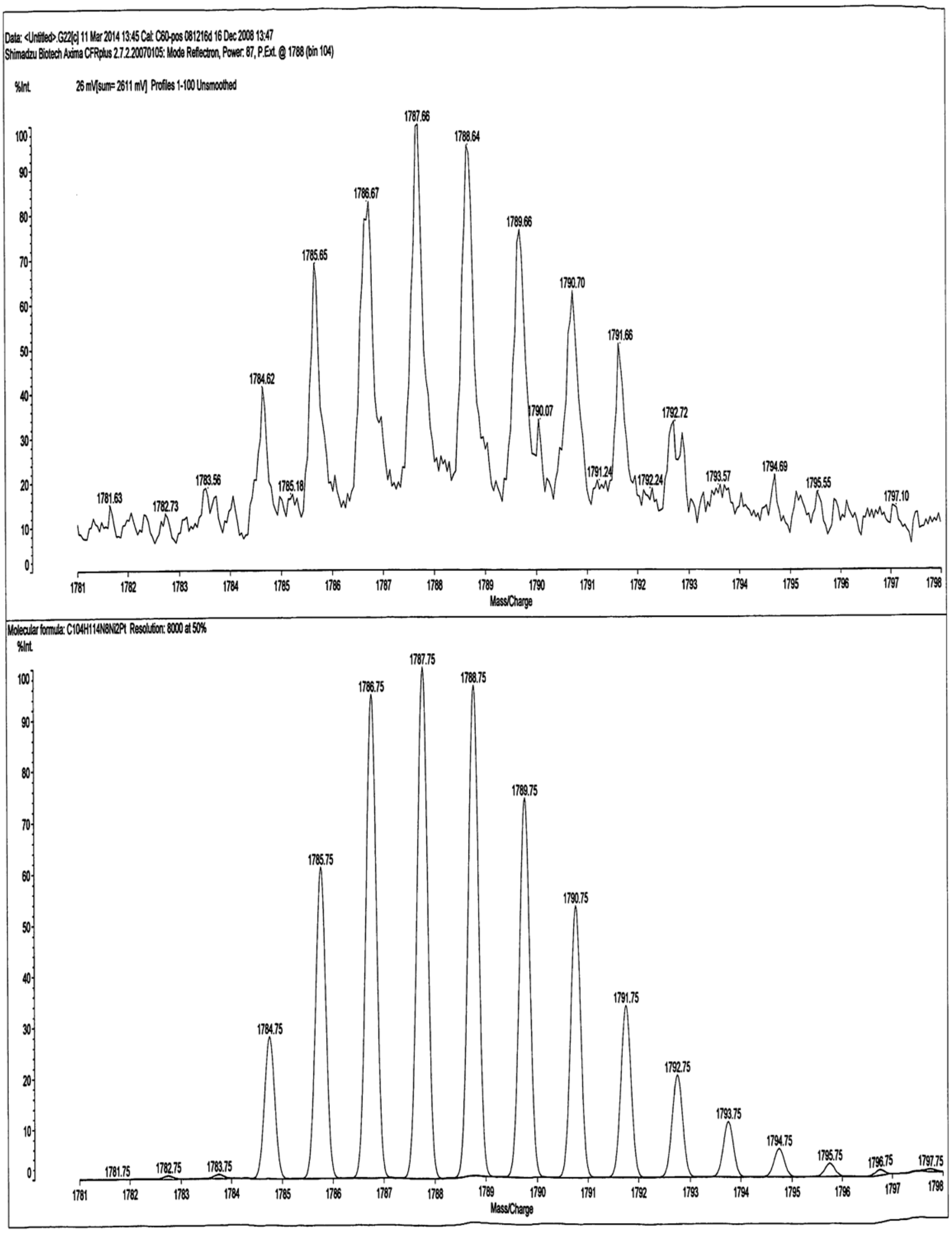

Figure S4-3. Simulated (bottom) and observed (top) MALDI-TOF-MS of **2Ni**.

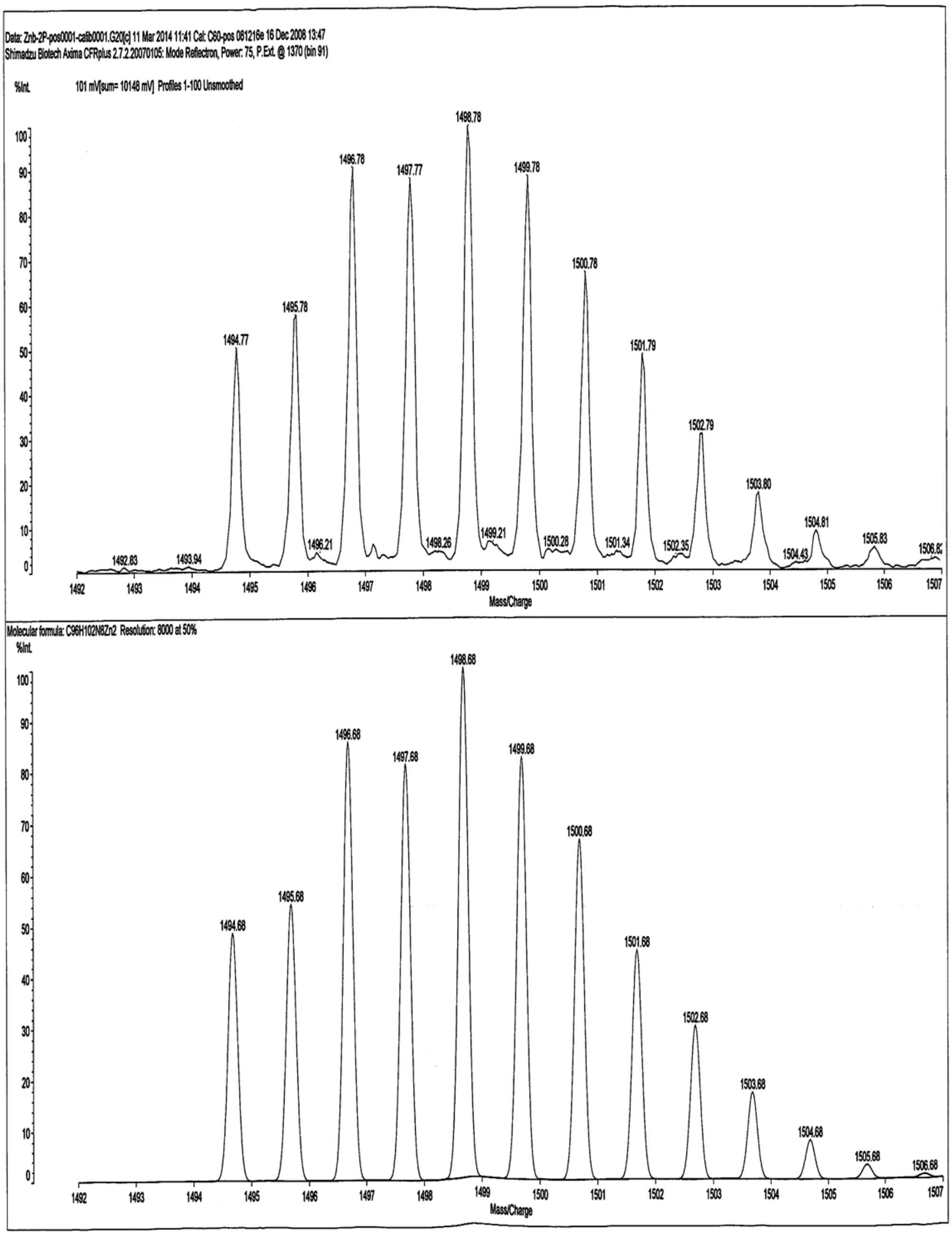

Figure S4-4. Simulated (bottom) and observed (top) MALDI-TOF-MS of **3Zn**.

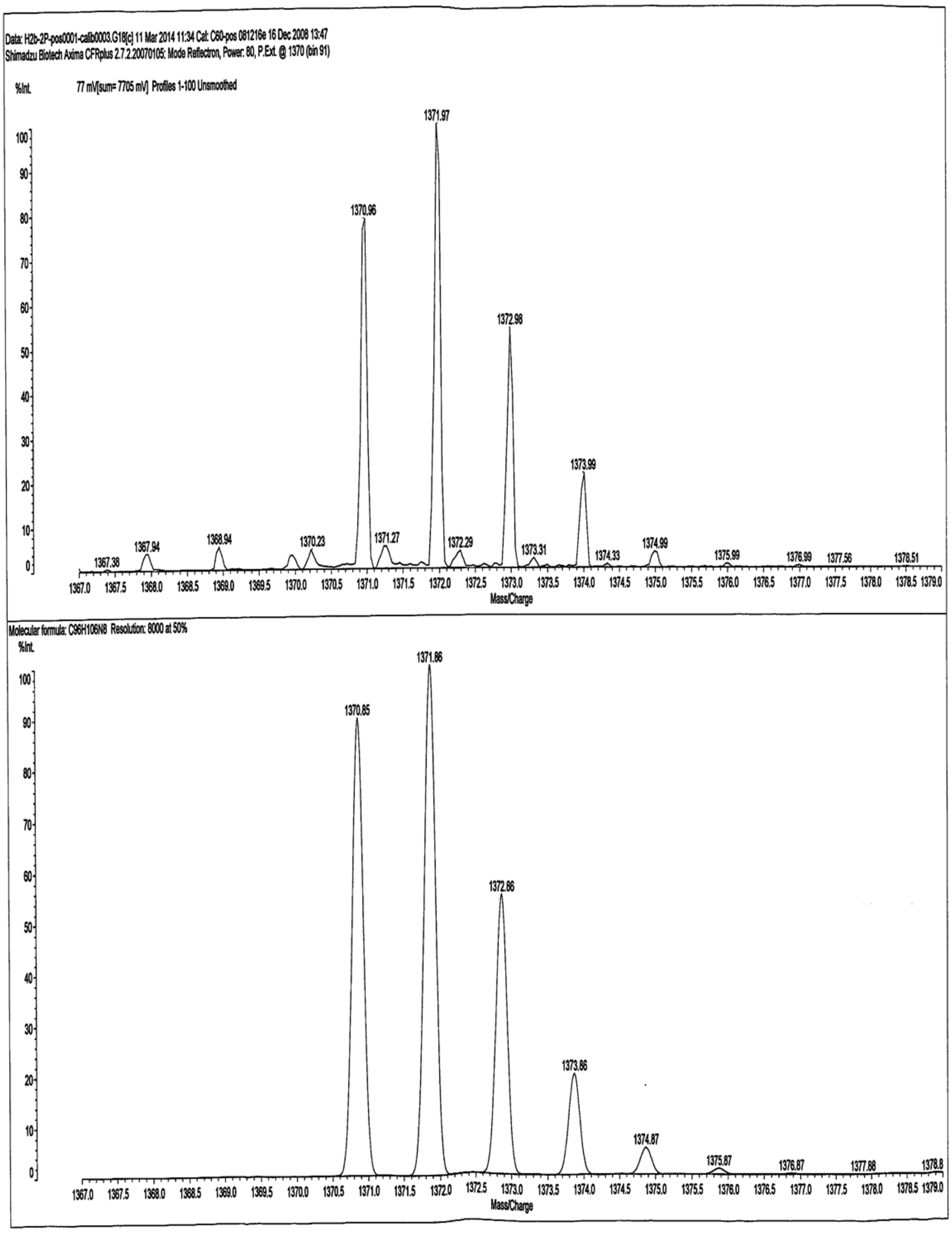

Figure S4-5. Simulated (bottom) and observed (top) MALDI-TOF-MS of **3H**.

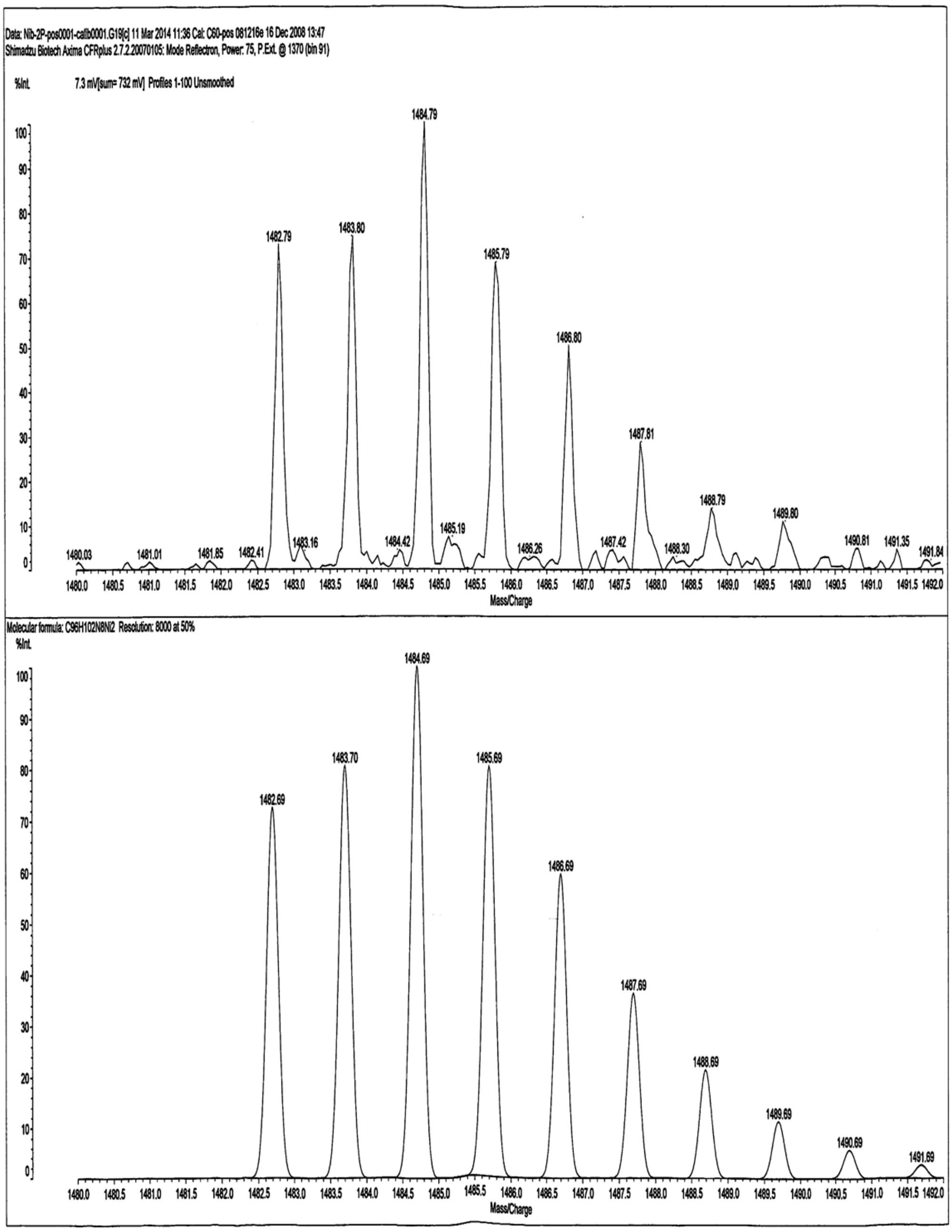

Figure S4-6. Simulated (bottom) and observed (top) MALDI-TOF-MS of **3Ni**.

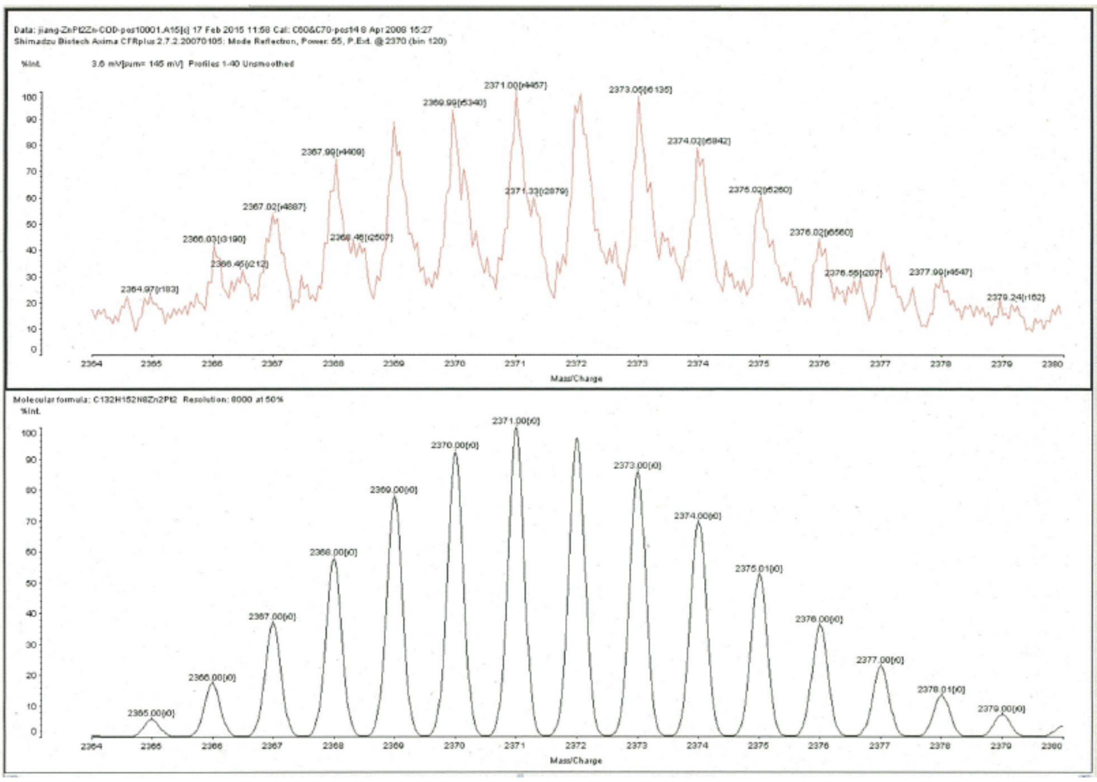

Figure S4-7. Simulated (bottom) and observed (top) MALDI-TOF-MS of **5Zn**.

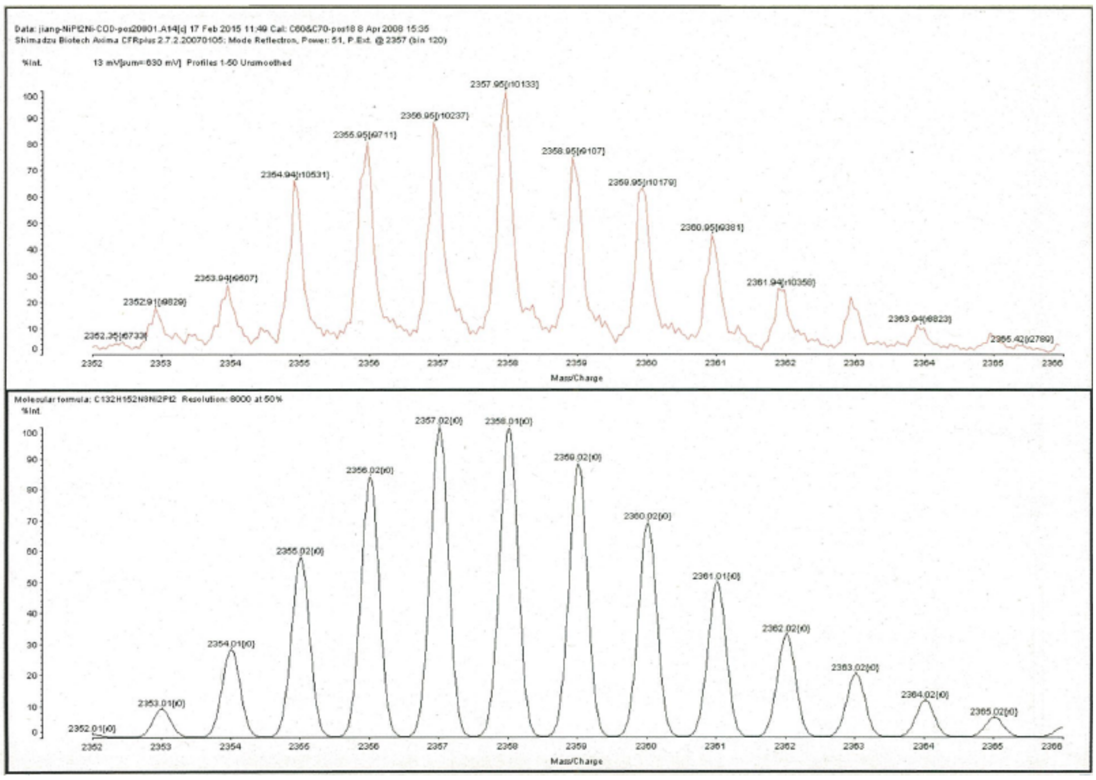

Figure S4-8. Simulated (bottom) and observed (top) MALDI-TOF-MS of **5Ni**.

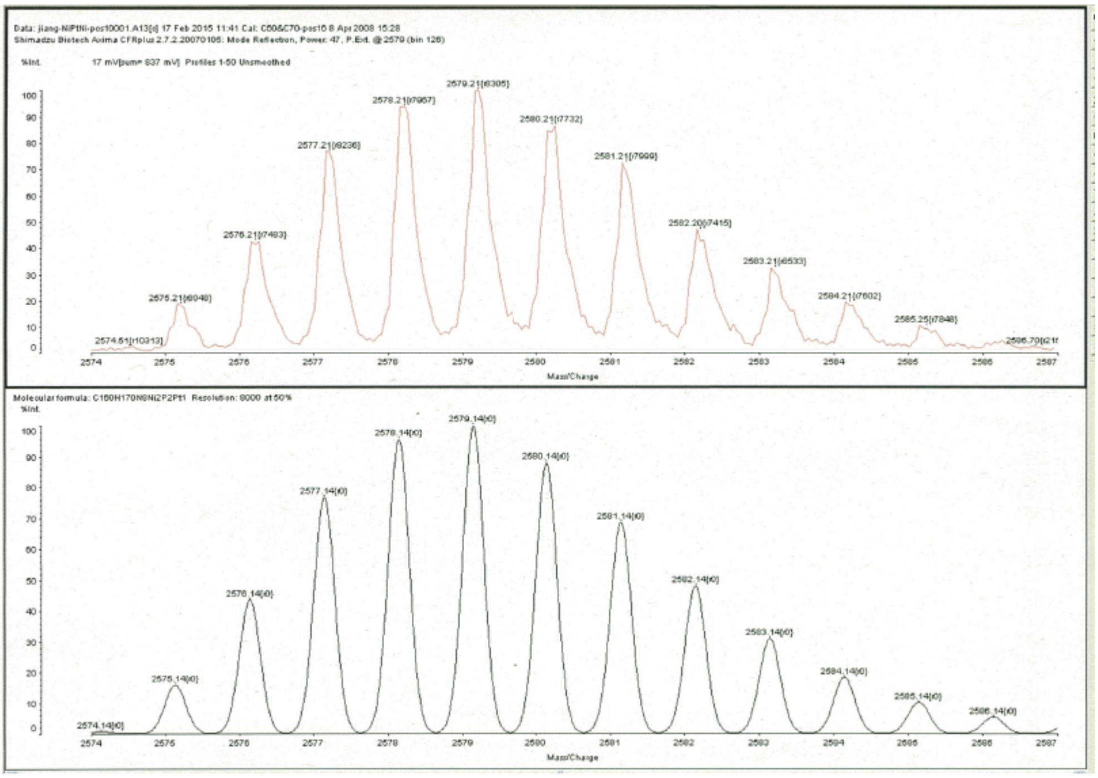

Figure S4-9. Simulated (bottom) and observed (top) MALDI-TOF-MS of **6Ni**.

5. X-Ray Crystallographic Details

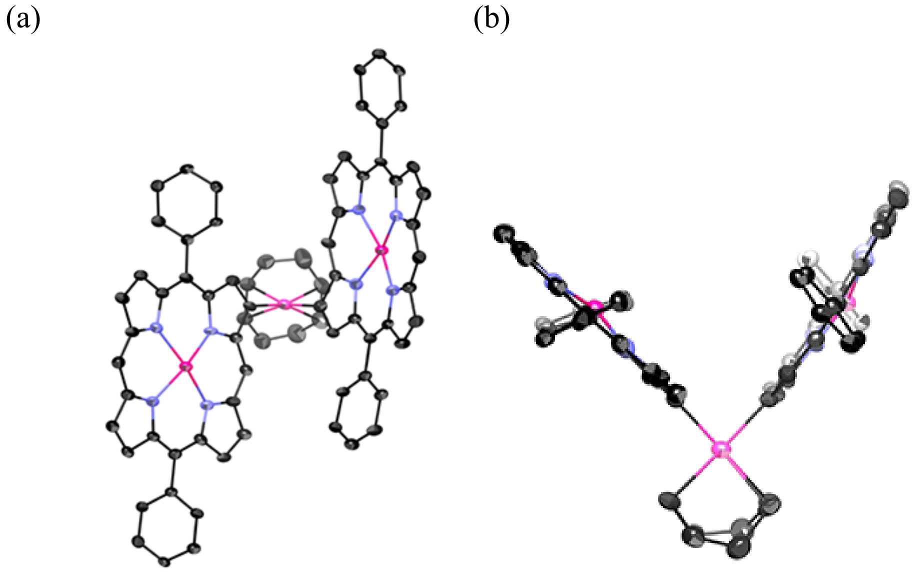

Figure S5-1. X-ray crystal structure of **2Zn**. (a) Top view. (b) Side view. Thermal ellipsoids were scaled to 30% probability. *tert*-Butyl groups, hydrogen atoms and solvent molecules were omitted for clarity.

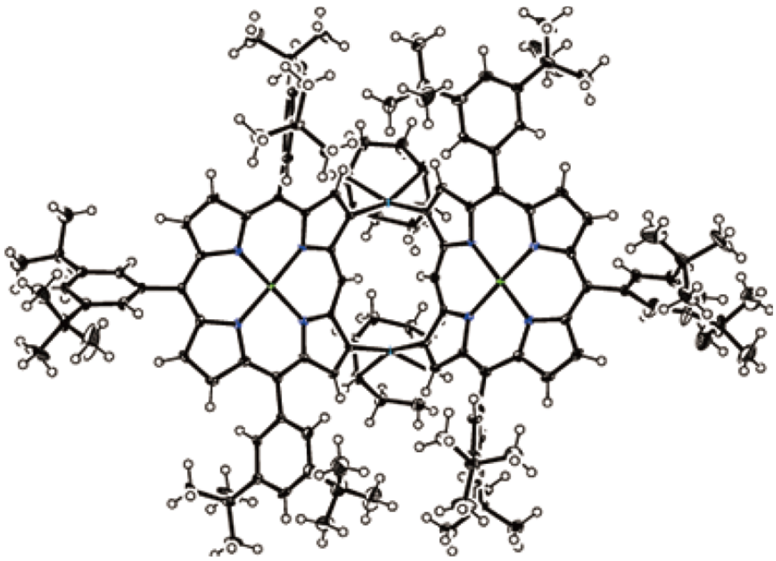

Figure S5-2. X-ray crystal structure of **5Ni**. (a) Top view. (b) Side view. Thermal ellipsoids were scaled to 30% probability. *tert*-Butyl groups, hydrogen atoms and solvent molecules were omitted for clarity.

*Explanation for a "level A" alert: The alert comes from the rotational disorder of *tert*-Butyl groups.

Table S5-1. Crystal data and structure refinements for **2Zn**, **2H**, **3Zn**, **5Ni** and **6Ni**.

Compound	**2Zn**	**2H**	**3Zn**	**5Ni**	**6Ni**
Empirical Formula	$C_{106}H_{120}N_8O_2Pt_1Zn_2 \cdot 3(CHCl_3) \cdot 2(CO)$	$C_{104}H_{118}N_8Pt \cdot 2(CHCl_3)$	$C_{106}H_{112}N_{10}Zn_2(CHCl_3)$	$C_{140}H_{162}N_8Ni_2Pt_2 \cdot 7.3(CHCl_3)$	$C_{160}H_{170}N_8Ni_2P_2Pt \cdot 4(CHCl_3) \cdot 0.8(CO) \cdot 0.2(O)$
M_W	2278.05	1913.89	1776.20	3336.17	3082.57
Crystal System	Triclinic	Monoclinic	Monoclinic	Triclinic	Monoclinic
Space Group	*P*-1 (No.2)	$P2_1/c$ (No.14)	*C* 2/*c* (No.15)	*P*-1 (No.2)	*C* 2/*c* (No.15)
a [Å]	14.8426(3)	20.8774(6)	31.53(1)	19.4832(10)	64.086(14)
b [Å]	20.1100(4)	15.8099(5)	8.731(2)	20.2466(16)	12.967(3)
c [Å]	21.2677(4)	30.4880(9)	36.552(13)	21.267(3)	40.547(8)
α [deg]	63.3696(7)	90	90	86.76(2)	90
β [deg]	78.2695(7)	99.1261(18)	113.582(11)	81.40(2)	102.600(5)
γ [deg]	71.6398(7)	90	90	67.434(11)	90
Volume [$Å^3$]	5371.33(18)	9935.8(5)	9222(5)	7659.6(12)	32884(12)
Z	2	4	4	2	8
Density [Mg/m^3]	1.409	1.279	1.279	1.446	1.245
Completeness	0.976	0.996	0.979	0.971	0.974
Goodness-of-fit	1.011	1.003	1.000	1.060	1.021
R_1 [$I > 2\sigma(I)$]	0.0791	0.0707	0.0553	0.0685	0.0947
wR_2 [$I > 2\sigma(I)$]	0.2151	0.1632	0.1470	0.1561	0.2538
R_1 (all data)	0.0946	0.0946	0.0754	0.0701	0.1095
wR_2 (all data)	0.2363	0.1792	0.1642	0.1570	0.2710
CCDC	1406330	1406329	1406343	1406331	1406332

Crystals suitable for single-crystal X-ray diffraction analysis were obtained by slow solvent diffusion of methanol into their respective solutions in chloroform. In the case of **3Zn**, a drop of pyridine was added to its chloroform solution.

6. Cyclic Voltammograms

(a)

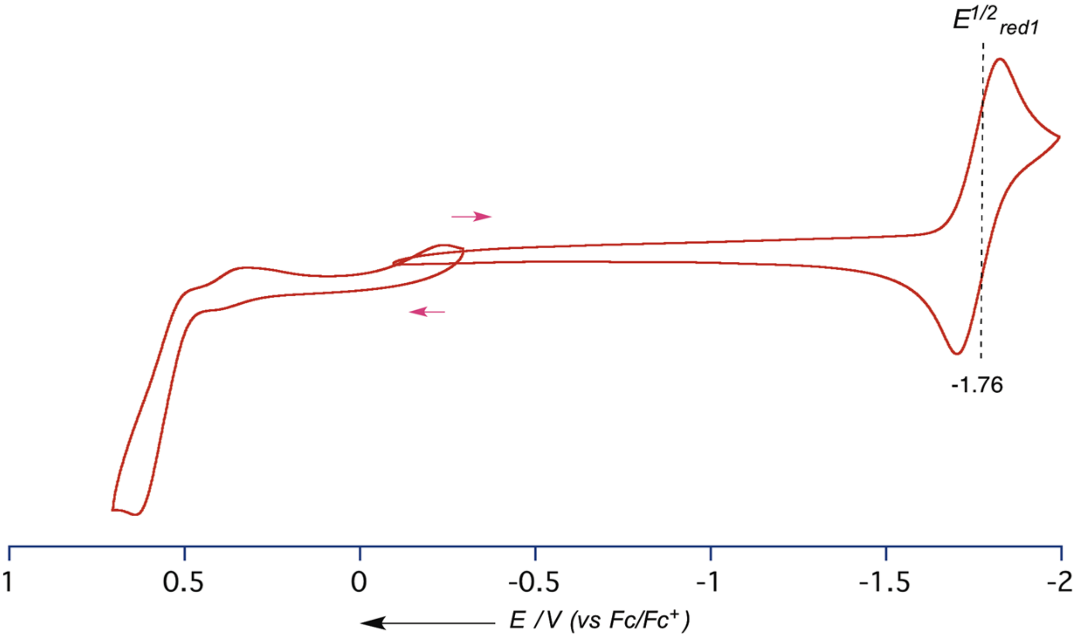

(b)

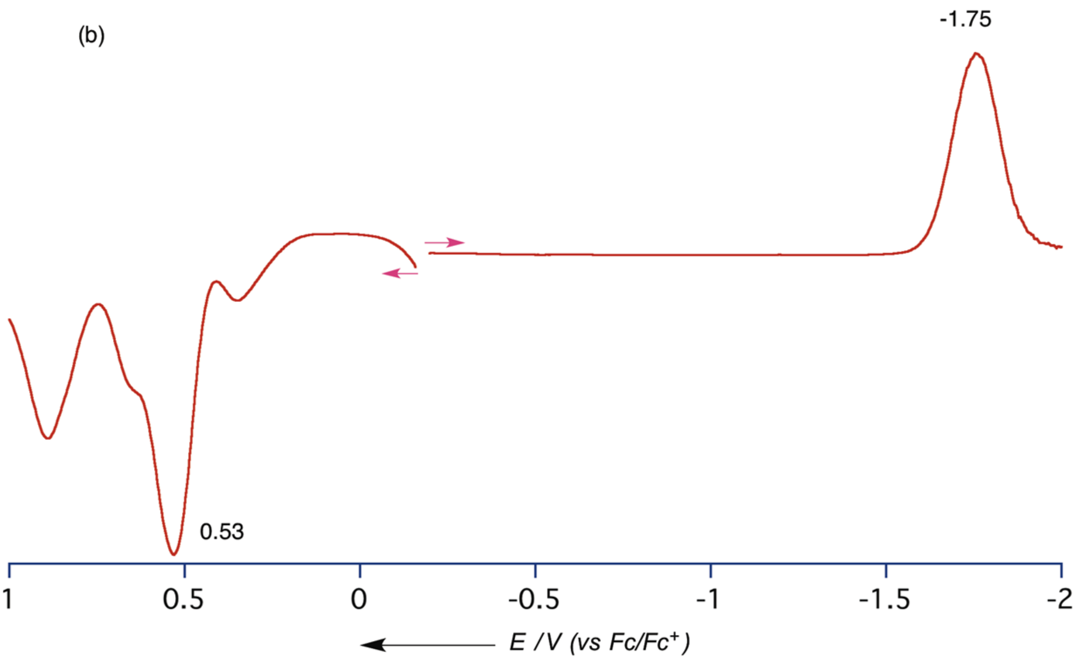

Figure S6-1. (a) Cyclic voltammogram and (b) differential-pulse voltammogram of Ni^{II} porphyrin (**Ni1**) measured in benzonitrile.

*It is known that 5,15-diarylporphyrinatonickel(II) undergoes electrochemical oxidation to form oligomers, that may cause irreversible oxidation waves.[S5]

(a)

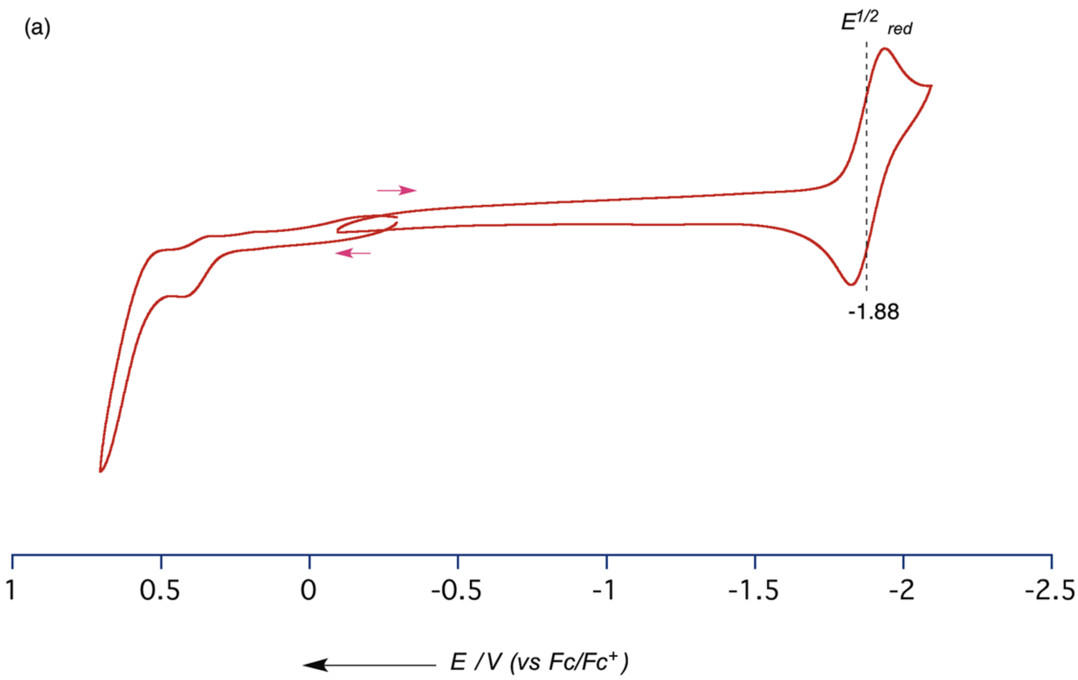

(b)

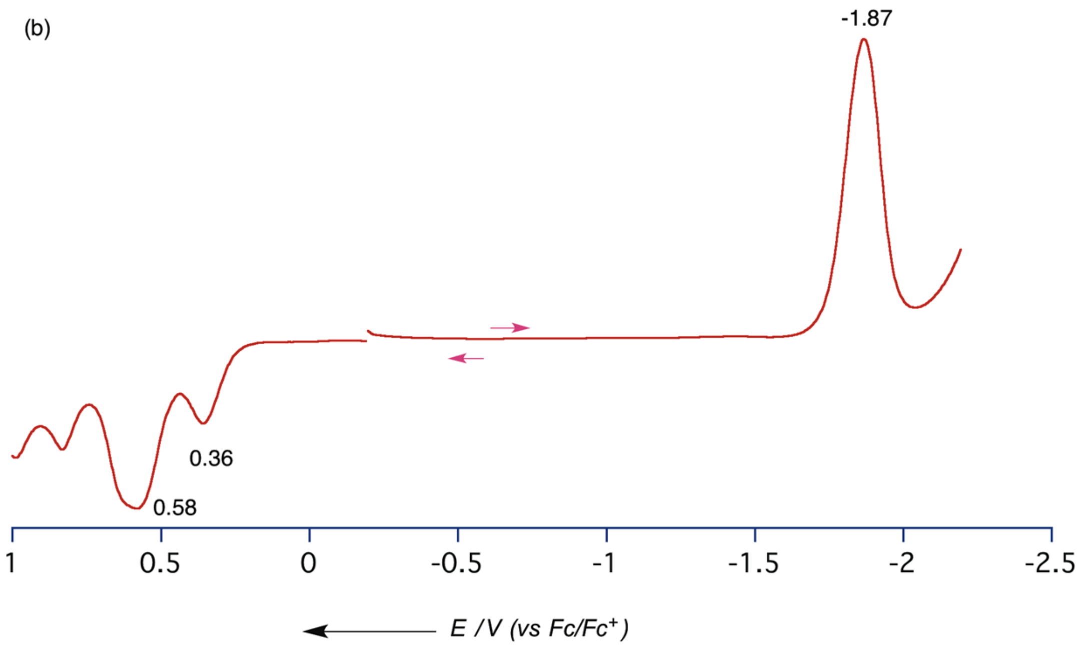

Figure S6-2. (a) Cyclic voltammogram and (b) differential-pulse voltammogram of **2Ni** measured in benzonitrile.

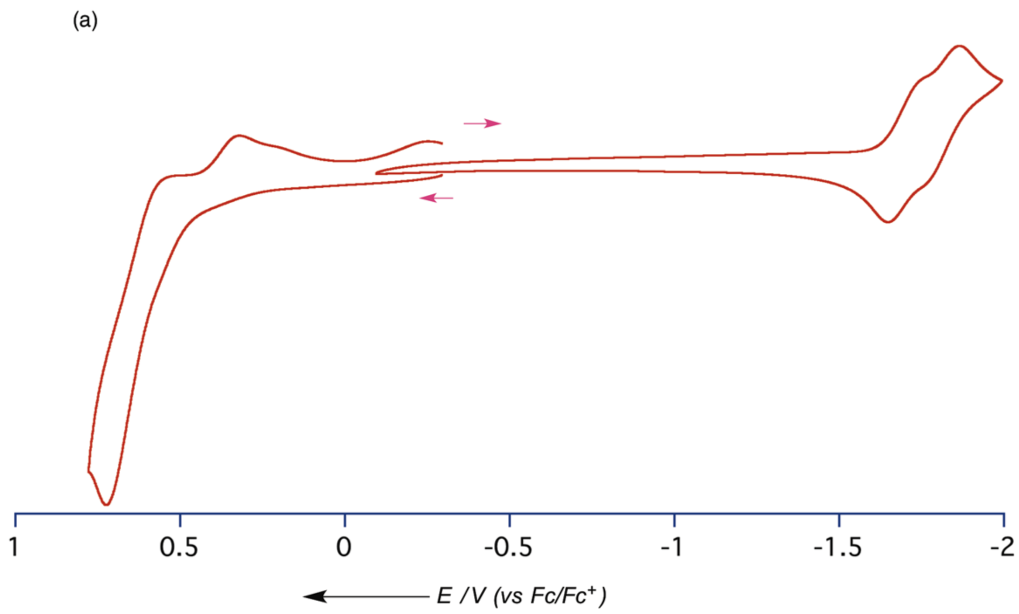

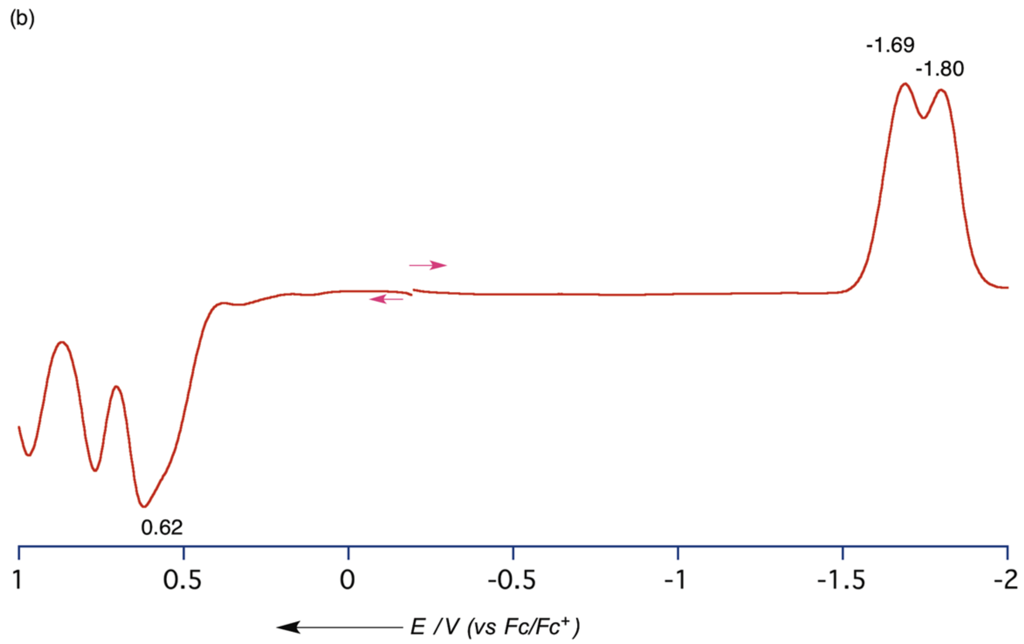

Figure S6-3. (a) Cyclic voltammogram and (b) differential-pulse voltammogram of **3Ni** measured in benzonitrile.

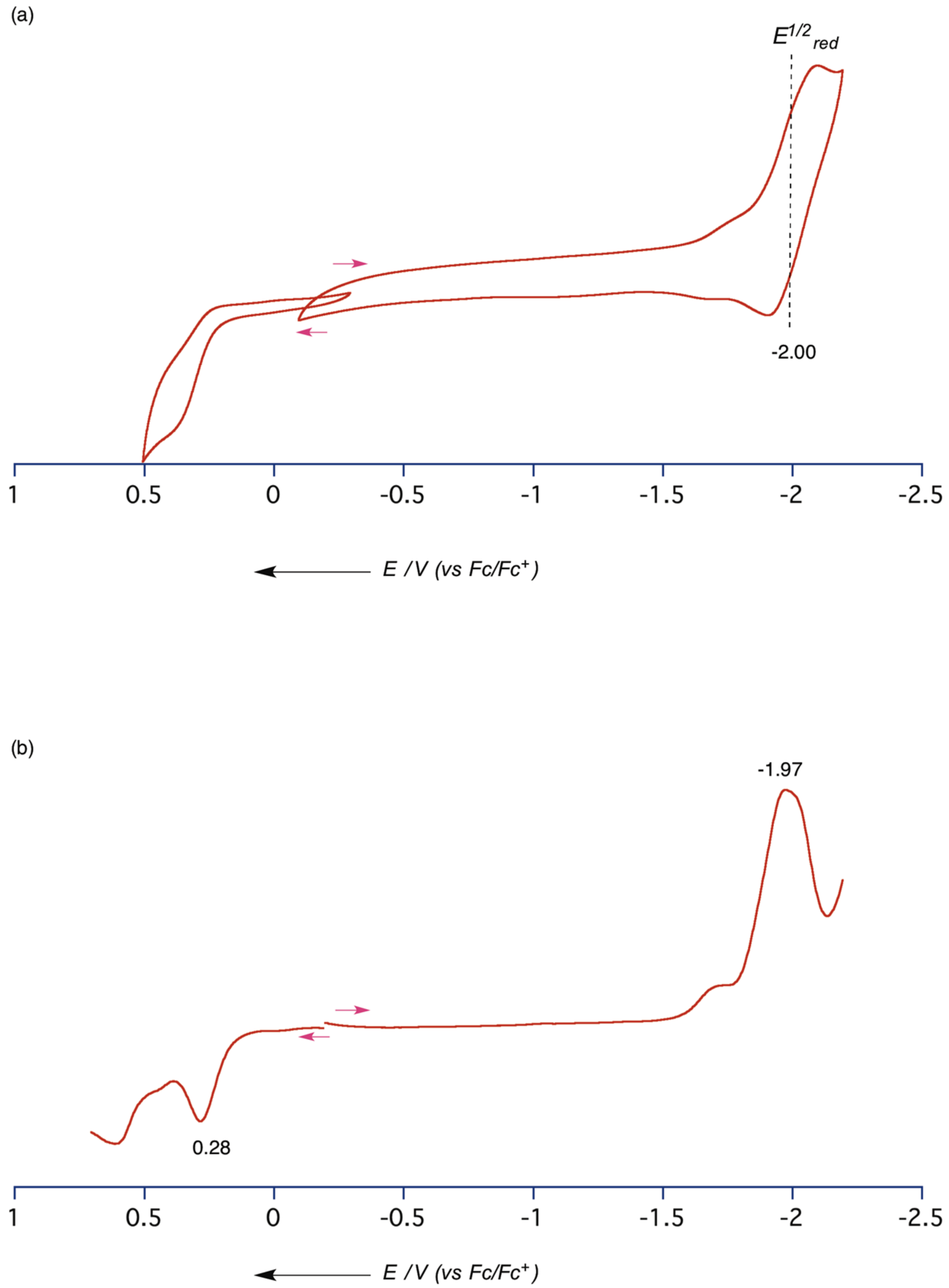

Figure S6-4. (a) Cyclic voltammogram and (b) differential-pulse voltammogram of **5Ni** measured in benzonitrile.

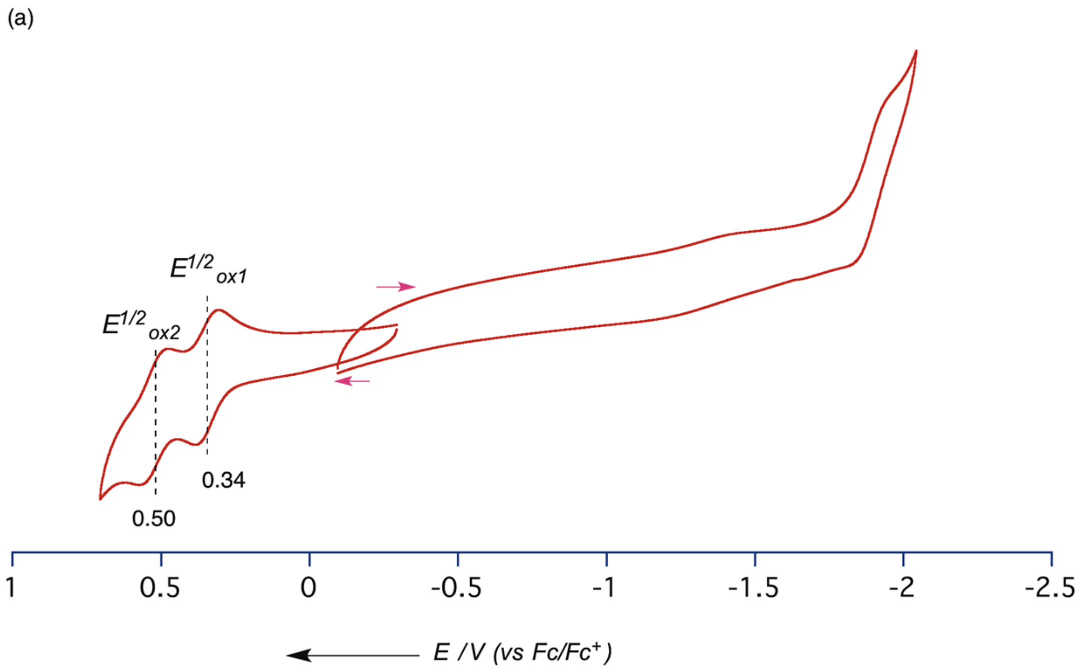

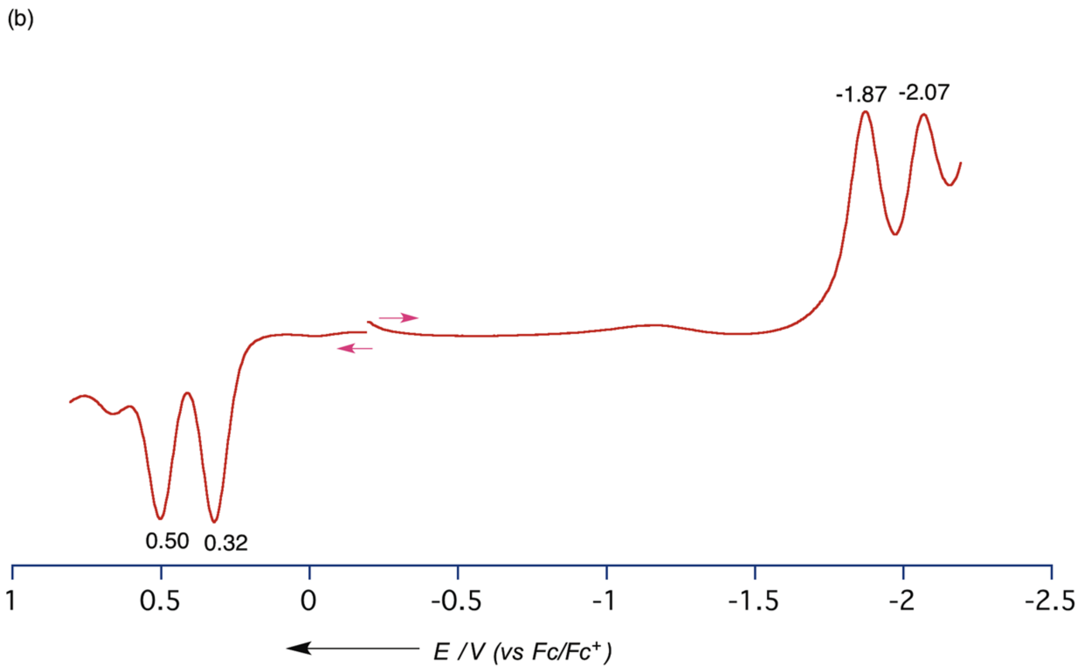

Figure S6-5. (a) Cyclic voltammogram and (b) differential-pulse voltammogram of **6Ni** measured in benzonitrile.

Table S6-1. Summary of the electrochemical potentials. The potentials were determined by cyclic voltammetry (CV) and differential-pulse voltammetry (DPV) as shown in Figure S6-1–S6-4. The potentials [V] were determined vs ferrocene/ferrocenium ion couple by CV or DPV in 0.1 M Bu_4NPF_6 in benzonitrile. Working electrode: Pt. Counter electrode: Pt wire. Reference electrode: $Ag/AgClO_4$. Scan rate: 0.05 V/s.

	$E^{1/2}_{ox2}$	$E^{1/2}_{ox1}$	$E^{1/2}_{red1}$	$E^{1/2}_{red2}$	ΔE_{HL}
Ni1[a]		0.53[b]	–1.76		2.29
2Ni		0.36[b]	–1.87		2.23
3Ni		0.62[b]	–1.69	–1.80	2.31
5Ni		0.28[b]	–1.97		2.25
6Ni	0.50	0.32	–1.87	–2.07[b]	2.19

[a] 5,15-Bis(3,5-di-*tert*-butylphenyl)porphyrinatonickel(II). [b] Irreversible peak.

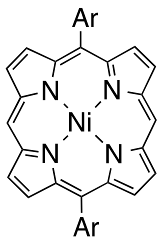

Ar = 3,5-di-*tert*-butylphenyl

Ni1

7. UV/Vis Absorption and Fluorescence Spectra

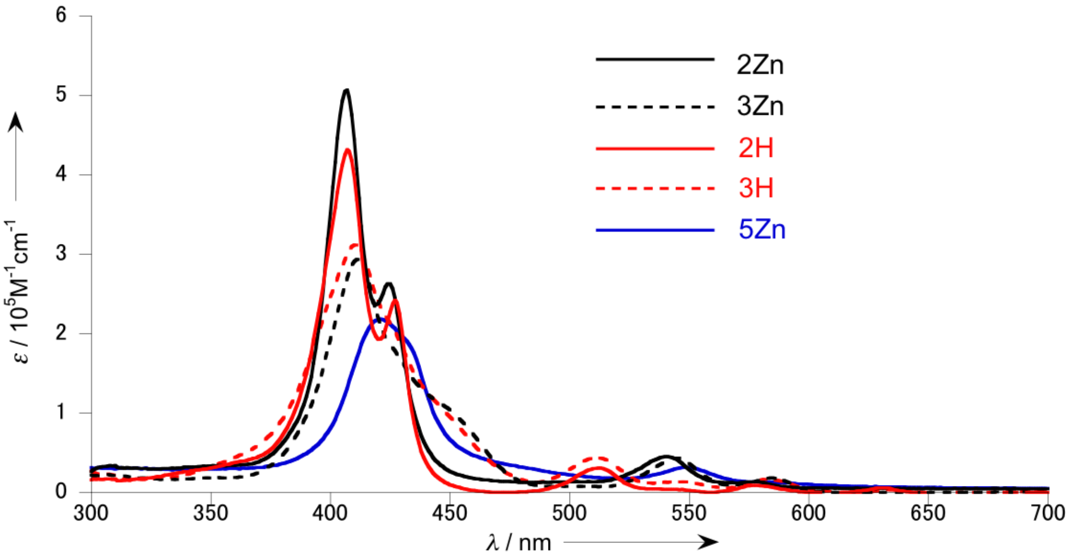

Figure S7-1. UV/Vis absorption spectra of **2Zn**, **2H**, **3Zn**, **3H**, and **5Zn** in CH_2Cl_2.

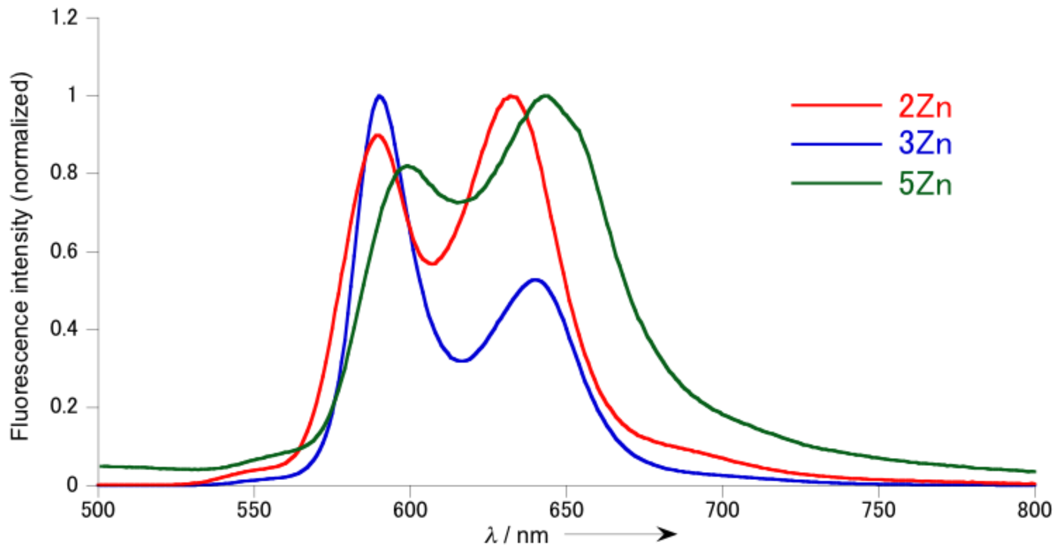

Figure S7-2. UV/Vis absorption and fluorescence spectra of **2Zn**, **3Zn** and **5Zn** in CH_2Cl_2.

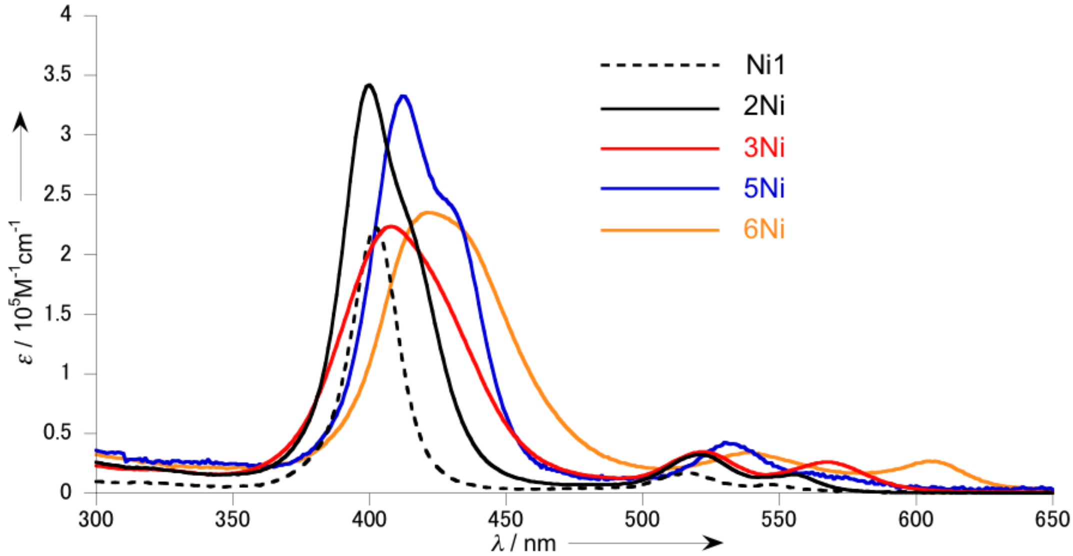

Figure S7-3. UV/Vis absorption spectra of **2Ni**, **3Ni**, **5Ni**, **6Ni** and **Ni1** in CH_2Cl_2.

8. DFT Calculations

All calculations were carried out using the *Gaussian 09* program.[S6] Initial geometries were obtained from X-ray structures and 3,5-di-*tert*-butylphenyl groups were replaced with hydrogen atoms or phenyl groups to reduce the calculation costs. Calculations were performed by the density functional theory (DFT) method with restricted B3LYP (Becke's three-parameter hybrid exchange functionals and the Lee-Yang-Parr correlation functional)[S7] level, employing basis sets 6-31G(d) for C, N, H, and P, and LANL2DZ for Ni and Pt.

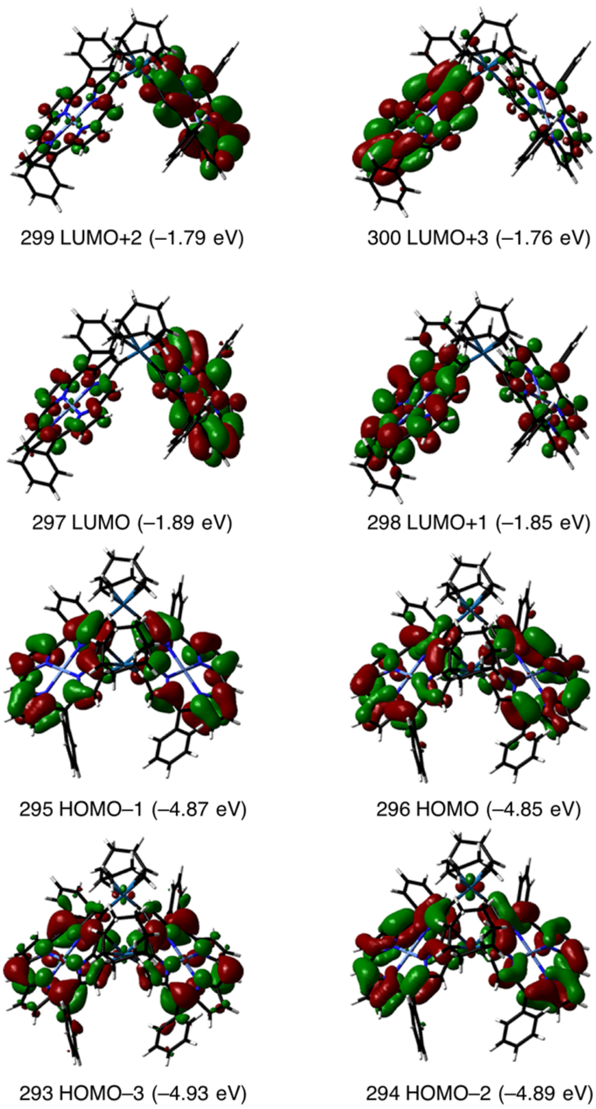

Figure S8-1. Kohn-Sham representations of the molecular orbitals of **2Ni**.

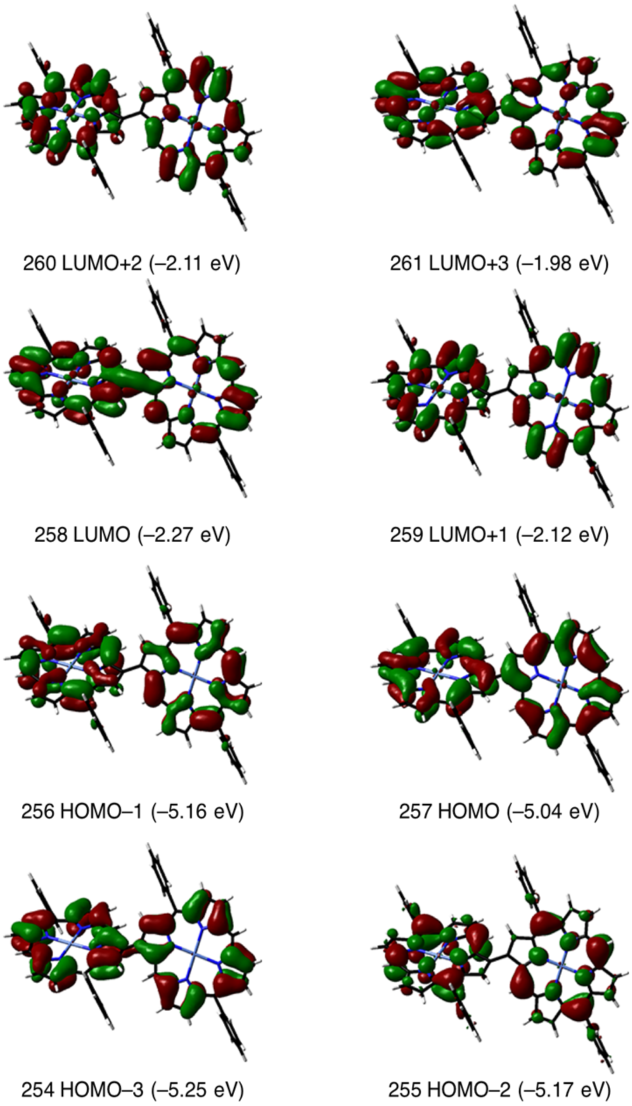

Figure S8-2. Kohn-Sham representations of the molecular orbitals of **3Ni**.

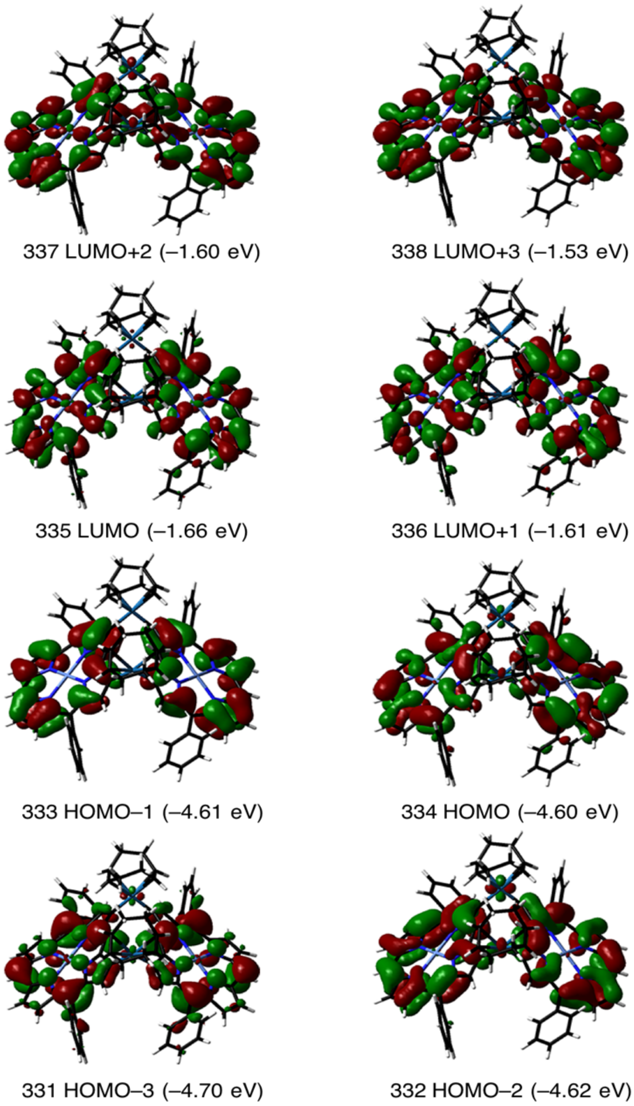

Figure S8-3. Kohn-Sham representations of the molecular orbitals of **5Ni**.

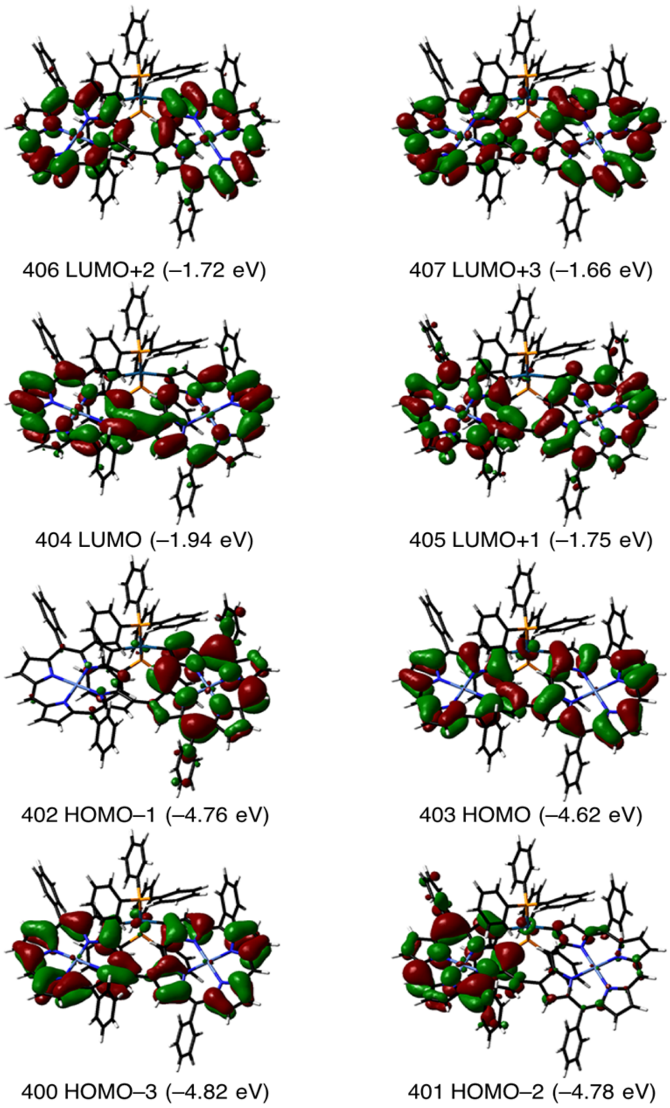

Figure S8-4. Kohn-Sham representations of the molecular orbitals of **6Ni**.

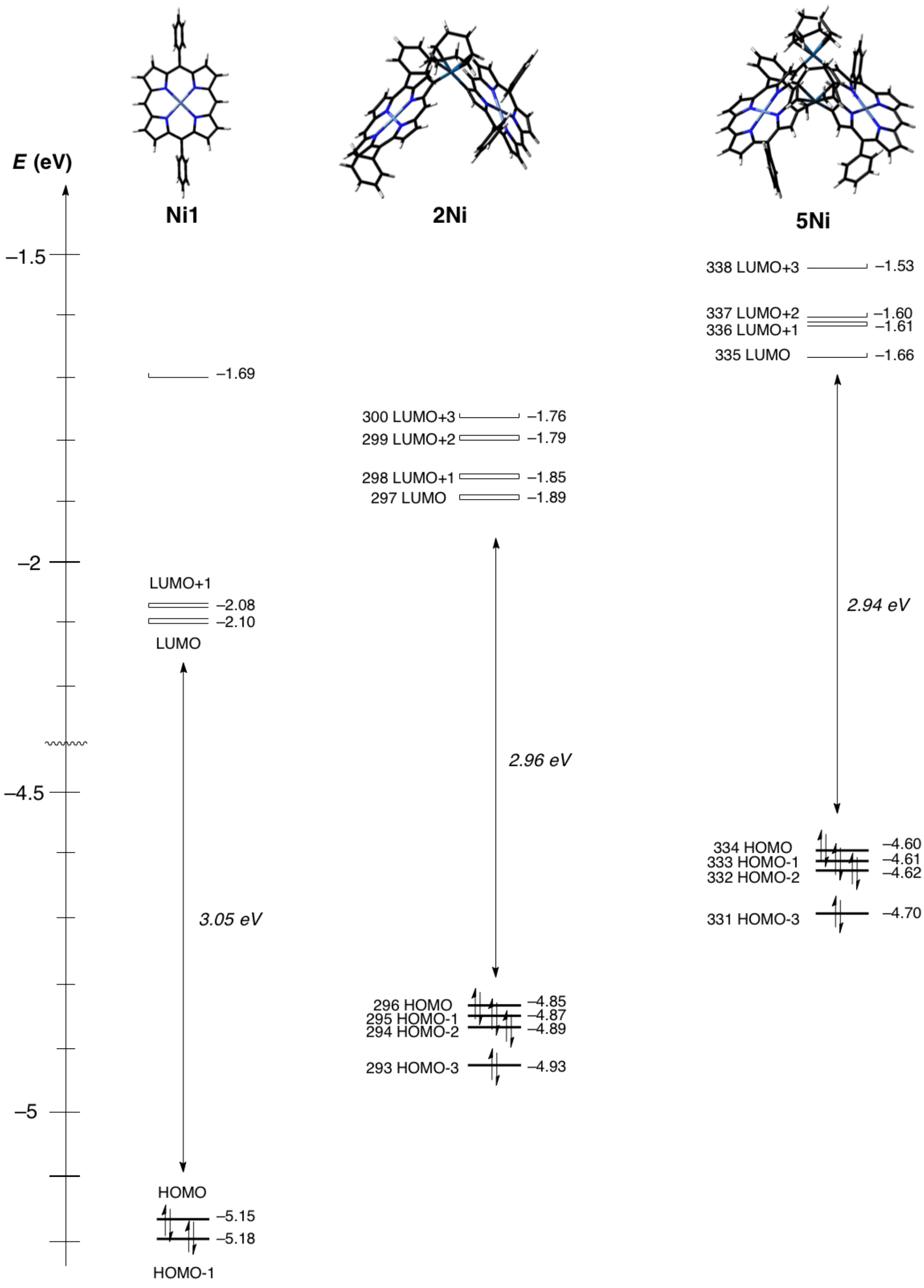

Figure S8-5. MO diagrams of **Ni1**, **2Ni**, and **5Ni**.

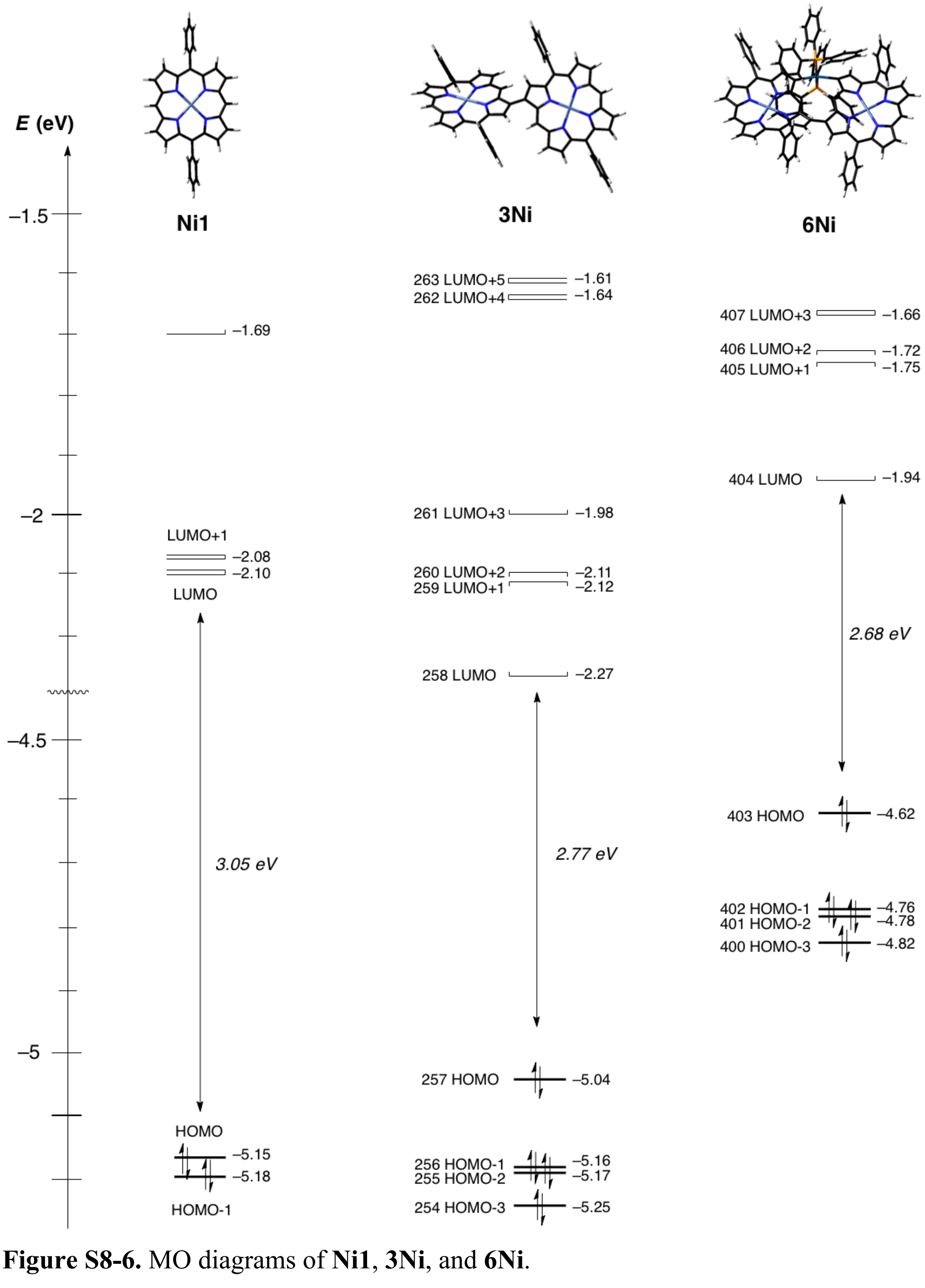

Figure S8-6. MO diagrams of **Ni1**, **3Ni**, and **6Ni**.

9. Supporting References

[S1] H. Hata, H. Shinokubo and A. Osuka, *J. Am. Chem. Soc.,* 2005, **127**, 8264.

[S2] H.-W Jiang, T. Tanaka, H. Mori, K. H. Park, D. Kim and A. Osuka, *J. Am. Chem. Soc.,* 2015, **137**, 2219.

[S3] Q. Hao, Y. Zeng, T. Yu, J. Chen, G. Yang and Y. Li, *Chem. Asian J.,* 2013, **8**, 1015.

[S4] K. Fujimoto, H. Yorimitsu and A. Osuka, *Org. Lett.,* 2014, **16**, 972.

[S5] T. Ogawa, Y. Nishimoto, N. Yoshida, N. Ono and A. Osuka, *Angew. Chem., Int. Ed*., 1999, **38**, 176.

[S6] Gaussian 09, Revision A.02, M. J. Frisch, G. W. Trucks, H. B. Schlegel, G. E. Scuseria, M. A. Robb, J. R. Cheeseman, G. Scalmani, V. Barone, B. Mennucci, G. A. Petersson, H. Nakatsuji, M. Caricato, X. Li, H. P. Hratchian, A. F. Izmaylov, J. Bloino, G. Zheng, J. L. Sonnenberg, M. Hada, M. Ehara, K. Toyota, R. Fukuda, J. Hasegawa, M. Ishida, T. Nakajima, Y. Honda, O. Kitao, H. Nakai, T. Vreven, J. A. Montgomery, Jr., J. E. Peralta, F. Ogliaro, M. Bearpark, J. J. Heyd, E. Brothers, K. N. Kudin, V. N. Staroverov, R. Kobayashi, J. Normand, K. Raghavachari, A. Rendell, J. C. Burant, S. S. Iyengar, J. Tomasi, M. Cossi, N. Rega, J. M. Millam, M. Klene, J. E. Knox, J. B. Cross, V. Bakken, C. Adamo, J. Jaramillo, R. Gomperts, R. E. Stratmann, O. Yazyev, A. J. Austin, R. Cammi, C. Pomelli, J. W. Ochterski, R. L. Martin, K. Morokuma, V. G. Zakrzewski, G. A. Voth, P. Salvador, J. J. Dannenberg, S. Dapprich, A. D. Daniels, Ö. Farkas, J. B. Foresman, J. V. Ortiz, J. Cioslowski and D. J. Fox, Gaussian, Inc., Wallingford CT, 2009.

[S7] (a) A. D. Becke, *J. Chem. Phys.,* 1993, **98**, 1372; (b) C. Lee, W. Yang and R. G. Parr *Phys. Rev. B,* 1998, **37**, 785.